ASSESSMENT REPORT TITLE PAGE AND SUMMARY

TITLE OF REPORT: 2017 Geophysical Report, Similkameen Canyon, Copper Mountain

TOTAL COST: $39,658

AUTHOR(S): **Peter Holbek**
SIGNATURE(S):

NOTICE OF WORK PERMIT NUMBER(S)/DATE(S): **(M29)**
STATEMENT OF WORK EVENT NUMBER(S)/DATE(S): **5696066 2018/May/03; 5691206 2018/Mar/27**

YEAR OF WORK: **2016/2017**

PROPERTY NAME: **Copper Mountain Mine**

CLAIM NAME(S) (on which work was done): Simcol # 1 Fr., Simcol #2 Fr, RR Fr, Brian Fr, Penny No.1 Fr, Copper Bluff Fr, EM Fr, Elephant No. 1, Elephant No. 2Fr, Elephant no. 4, SER 15.

COMMODITIES SOUGHT: **Cu, Au, Ag**

MINERAL INVENTORY MINFILE NUMBER(S),IF KNOWN: 092HSE001 to 132

MINING DIVISION: **Kamloops**
NTS / BCGS: **92H/7E**
LATITUDE: **49° 20' 34"**
LONGITUDE: **120° 31' 47"** (at centre of work)
UTM Zone: **10** EASTING: **678200** NORTHING: **5468000**

OWNER(S): **Copper Mountain Mine B.C.**

MAILING ADDRESS: 550 **– 1700- 700 West Pender St, Vancouver, BC, V6C 1G8**

OPERATOR(S) [who paid for the work]: **Copper Mountain Mining Corp.**

MAILING ADDRESS: **As Above**

REPORT KEYWORDS (lithology, age, stratigraphy, structure, alteration, mineralization, size and attitude. (Do not use abbreviations or codes) **Nicola Group Volcanic Rocks, Lower Jurassic, Cu-Au Alkalic Porphyry, Alkalic and Potassic Alteration.**

REFERENCES TO PREVIOUS ASSESSMENT WORK AND ASSESSMENT REPORT NUMBERS: **35817,30945, 35176, 29220, 25377, 24041, 23864**

TYPE OF WORK IN THIS REPORT	EXTENT OF WORK (in metric units)	ON WHICH CLAIMS	PROJECT COSTS APPORTIONED (incl. support)
GEOLOGICAL (scale, area)			
Ground, mapping			
Photo interpretation			Included below
GEOPHYSICAL (line-kilometres)			
Ground			
Magnetic			
Electromagnetic			
Induced Polarization		Simcol # 1 Fr., Simcol #2 Fr, RR Fr, Brian Fr, Penny No.1 Fr, Copper Bluff Fr, EM Fr, Elephant No. 1, Elephant No. 2Fr, Elephant no. 4, SER 15	$29,525
Radiometric			
Seismic			
Airborne			
GEOCHEMICAL (number of samples analysed for …)			
Soil			
Silt			
Rock			
Other			
DRILLING (total metres, number of holes, size, storage location)			
RELATED TECHNICAL			
Mineralographic			
Metallurgic			
PROSPECTING (scale/area)			
PREPATORY / PHYSICAL			
Line/grid (km)			
Topo/Photogrammetric (scale, area)	12 Km2	As above + others	7,533
Legal Surveys (scale, area)			
Road, local access (km)/trail			
Trench (number/metres)			
Excavator test pits			
Other	Management, reports		$2600
		TOTAL COST	**$39,658**

Copper Mountain Project
Princeton, British Columbia

Volterra 2D and 3D Induced Polarization Survey, Similkameen Canyon Area

NTS Map Sheet 92H/7E
Latitude 49° 20'N; Longitude 120° 31'W

Prepared for Copper Mountain Mining Corp.

by
Peter Holbek
May 28th, 2016

Table of Contents

List of Figures

List of Tables

1. Introduction

1.1 Property Description and Location

The Copper Mountain Project is situated 15 km south of Princeton, British Columbia and 180 km east of Vancouver (Lat. 49 20' N; Long. 120 31' W). The NTS map sheet is 92H/7E, (Figure 1).

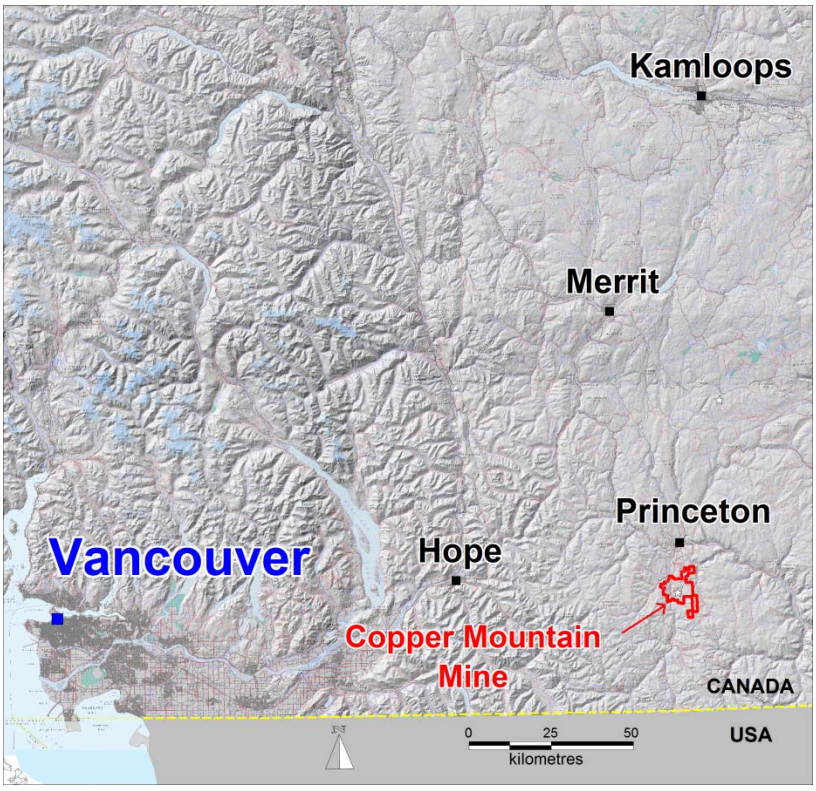

Figure 1.1: Property Location

The property consists of 135 Crown granted mineral claims, 132 located mineral claims, 14 mining leases, and 12 fee simple properties covering an area of 6,702.1 hectares or 67 square kilometres. Claims are shown in Figure 4.1 and listed in Appendix 1. Approximately 22% of the claims, primarily in the northwestern property area, are subject to production royalties of up to 5%. Known mineralization within the royalty areas includes the Virginia and Alabama deposits, of which only the Virginia deposit is permitted and currently within the mine plan.

CMMC owns 75% the project through its 100% ownership of Copper Mountain Mine (BC) Ltd. the other 25% of the project is owned by Mitsubishi Materials Corporation (MMC) of Japan. The claims straddle the Similkameen River with the Ingerbelle deposit on the west side of the river and the Copper Mountain deposits on the east side of the river (Figure 2). The Ingerbelle side of the property is immediately adjacent to the Hope-Princeton Highway (No. 3) and has numerous

roads from previous mining activity. The original mill complex is located on the Ingerbelle side and was connected to the Copper Mountain side by a conveyor system.

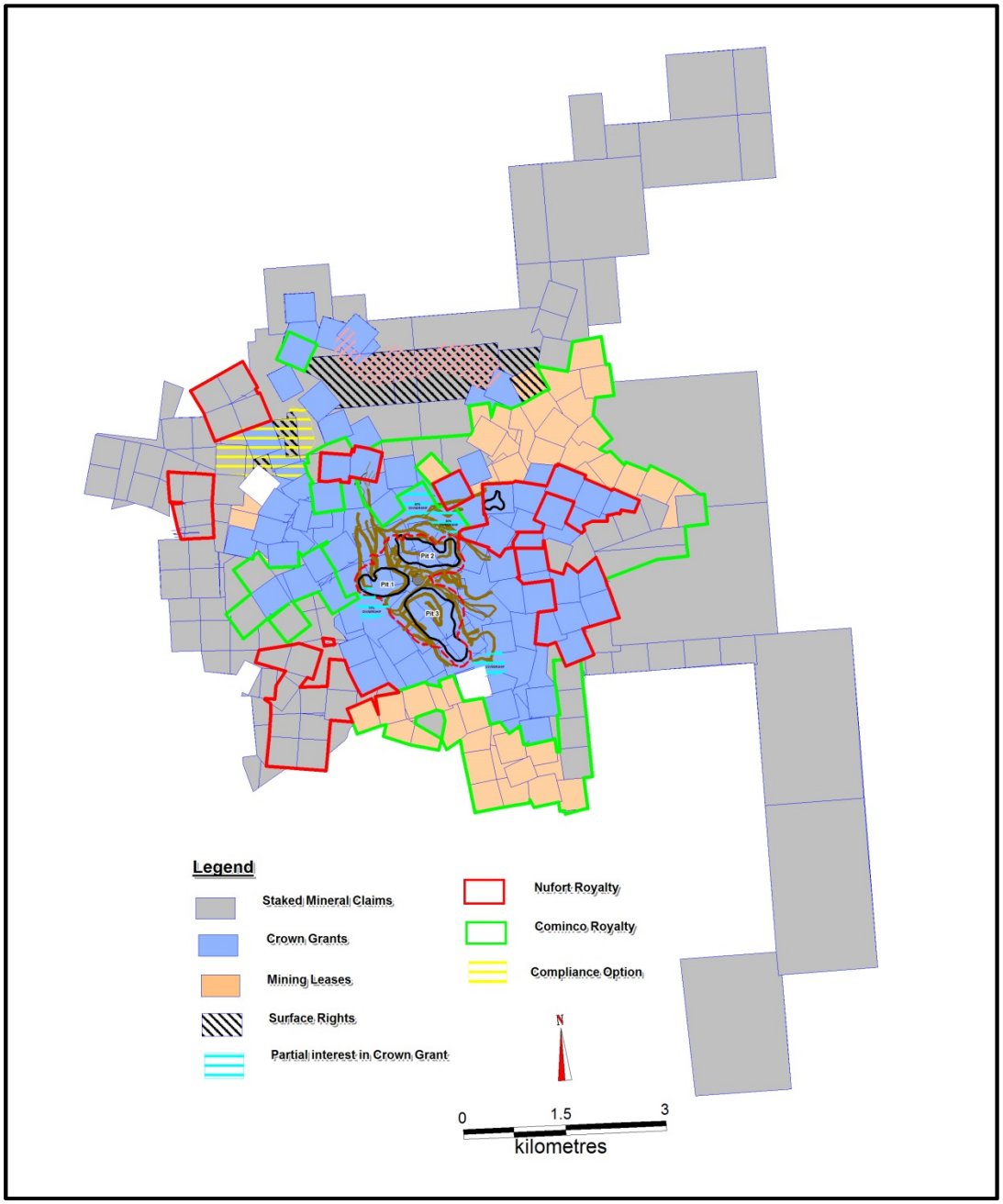

Figure 1.2: Claim Map for Copper Mountain Property.

Access to the Copper Mountain area is via a 28 km paved road from the town of Princeton. A significant part of the existing rock dumps adjacent to the Similkameen River at the mine site have been reclaimed. Envirogreen Technologies Ltd, a soil remediation company operates near the Ingerbelle Pit area and was previously spreading remediated sewage on the tailings as well as rock dumps which helps to provide a top soil for the establishment of various forms of plant life. Some of the reclaimed rock dumps are currently being used for grazing cattle.

The mine has a BC mining permit (MX-29) and has operated in compliance with all environmental and government regulations since start-up. An $8.0 million reclamation bond is attached to the property and this bond is posted with the BC Government as a requirement to cover current environmental liabilities.

1.2 Property, Accessibility, Climate and Physiograpy

Almost all of the property area is accessible by highways, paved access road and local gravel roads on the property remaining from previous mining activity. The nearest railway is at Hope some 120 km from the mill building. Grid power is connected to the property at the previous mill where it was sufficient to operate the 25,000 tpd concentrator and related infrastructure. Water for previous operations was pumped from the Similkameen River to make up that recycled and this permit is still active and is sufficient to support higher tonnage than the previous operation.

Topography is gentle to moderate over most of the plateau area of Copper Mountain, where elevations range from 1,050 m to 1,300 m, but becomes rugged in the Similkameen River Canyon. The elevation of the river is approximately 770 m and the canyon walls are steep.

The Copper Mountain area has a relatively dry climate, typical of the southern interior of British Columbia. Summers are typically warm and dry whereas the winters are cool with minor precipitation. Most of the precipitation during the winter months falls as snow with total snow fall of approximately 200 cm resulting in accumulated (compacted) snow depths of approximately 60-70 cm on the ground. Weather data from the mine-site has been collected from 1966 through to 1996. Temperatures range from an average annual high of 35^{o}C and the average annual low of -29.5^{o}C, with the annual mean temperature being 6 degrees. Total annual precipitation varies widely, ranging from a low of 253 mm to a high of 790 mm with the average being 400 mm. The bio-geoclimatic zones for the area are Ponderosa Pine - Bunch grass at the lower elevations, transitioning into Lodgepole Pine forests at the higher elevations.

The town of Princeton has a population of approximately 3,000 and has a diversified economy driven by ranching, forestry and tourism, although during the mine operation, Similco Mines was the predominate employer in the area. The town has services typical of its size; however the general proximity of Vancouver, 267 km to the west, allows many services to be obtained there.

Exploration and mining have been and may still be conducted year-round, due to the established roads and the projects proximity to the nearby towns. The property had sufficient surface rights for past operations however CMMC is reviewing the possibility that in future all infrastructure will be located on the east side of the Similkameen river as that is where the current exploration program is focused. Without detailed analysis, there appears to be sufficient land area to locate future plant, tailings and waste rock storage. There are numerous roads and space for any exploration programs. Three phase electric power comes onto the property via an existing 138KV power line at the old mill building.

1.4 Property History

Initial exploration at Copper Mountain dates back to 1884. A number of attempts at initiating production were made during the period from 1892 to 1922 but were unsuccessful. In 1923, Granby Consolidated Mining, Smelting and Power Company (Granby) acquired the property, built a milling facility in Allenby adjacent to Princeton and between 1925 and 1957, extracted 31.5 million tonnes of ore with a recovered grade of 1.08% copper from primarily underground operations. Subsequently, Newmont Mining Corporation began open pit operations at Ingerbelle in 1972 with an initial reserve of 67 million tons grading 0.55% copper. In 1979, development of mineable reserves on the Copper Mountain side of the project commenced with the installation of a new primary crusher and conveyer system across the Similkameen River. This helped feed the mill which been expanded from 13,500 tonnes per day to over 20,000 tpd. Production from the Copper mountain side was from pits 1, 2, and 3. The entire property was sold by Newmont in 1988 to Cassiar Mining Corporation (later to become Princeton Mining Corp. (PMC)). The operation continued under the name Similco Mines Ltd. with mining from pits 1 and 3 and a small tonnage from the Virginia pit, until late1996, when economic conditions prevented profitable operations and the mine closed.

Copper Mountain Mining Corporation was formed in 2006 and acquired the Copper Mountain Property and immediately embarked on a large exploration program. Following a period of historical data collection and verification, a Quantec Titan24 deep-penetration IP survey, and a re-interpretation of the data, an aggressive drill program was undertaken to expand the resource base. Drilling was successful and, following a Feasibility Study in 2009, a production decision was made for a 35,000t/d milling operation on the basis of a 211Mt reserve grading 0.37% Cu plus gold and silver, with a life of mine strip ratio of 2:1, and a resource base (including inferred

material) of ~5 billion pounds of copper. Mitsubishi Material s Corp., a long time purchaser of the concentrate from the site, partnered with CMMC by purchasing a 25% project interest and arranging 75:25% debt to equity financing at very attractive interest rates in exchange for a life of mine concentrate off-take agreement. Construction was initiated in 2010 and the first concentrate was produced in June, 2011. Concentrate is trucked to Vancouver for shipping to Mitsubishi's smelters in Asia. The mine has had difficulties consistently achieving design capacity due to problems getting very hard ore through the SAG mill. Production problems were partly mitigated by a combination of changes in the mine plan, to mining softer material and high intensity blasting. However, the addition of a large secondary crushing unit to the mill circuit between the primary crusher and the SAG mill has allowed the mill to consistently exceed design capacity and thereby lower production costs.

Although the mine has a large resource base, exploration is still on-going in an effort to continuously upgrade and improve resource and reserve status of the property.

1.5 Description of Current Exploration Work

The work documented in this report was carried out in late May to early June, 2017, and consisted of 7 geophysical survey lines, totalling 9,925m. The survey lines were run along both sides of the Similkameen Canyon between the area of current mining in the Copper Mountain Super pit, on the eastern side of the river, and previously mined Ingerbelle pit, on the western side of the Similkameen River. The geophysical survey was carried out by SJ Geophysics of Delta, B.C.

The objective of the geophysical survey was to determine if there was connection of the mineralization between the super-pit and Ingerbelle pit, as well as to search for possible extensions of the Ingerbelle mineralization. During the same time frame a Lidar Survey was undertaken over the Similkameen River canyon and general mine site. A structural interpretation of the geophysical survey area was carried out using Lidar imaging.

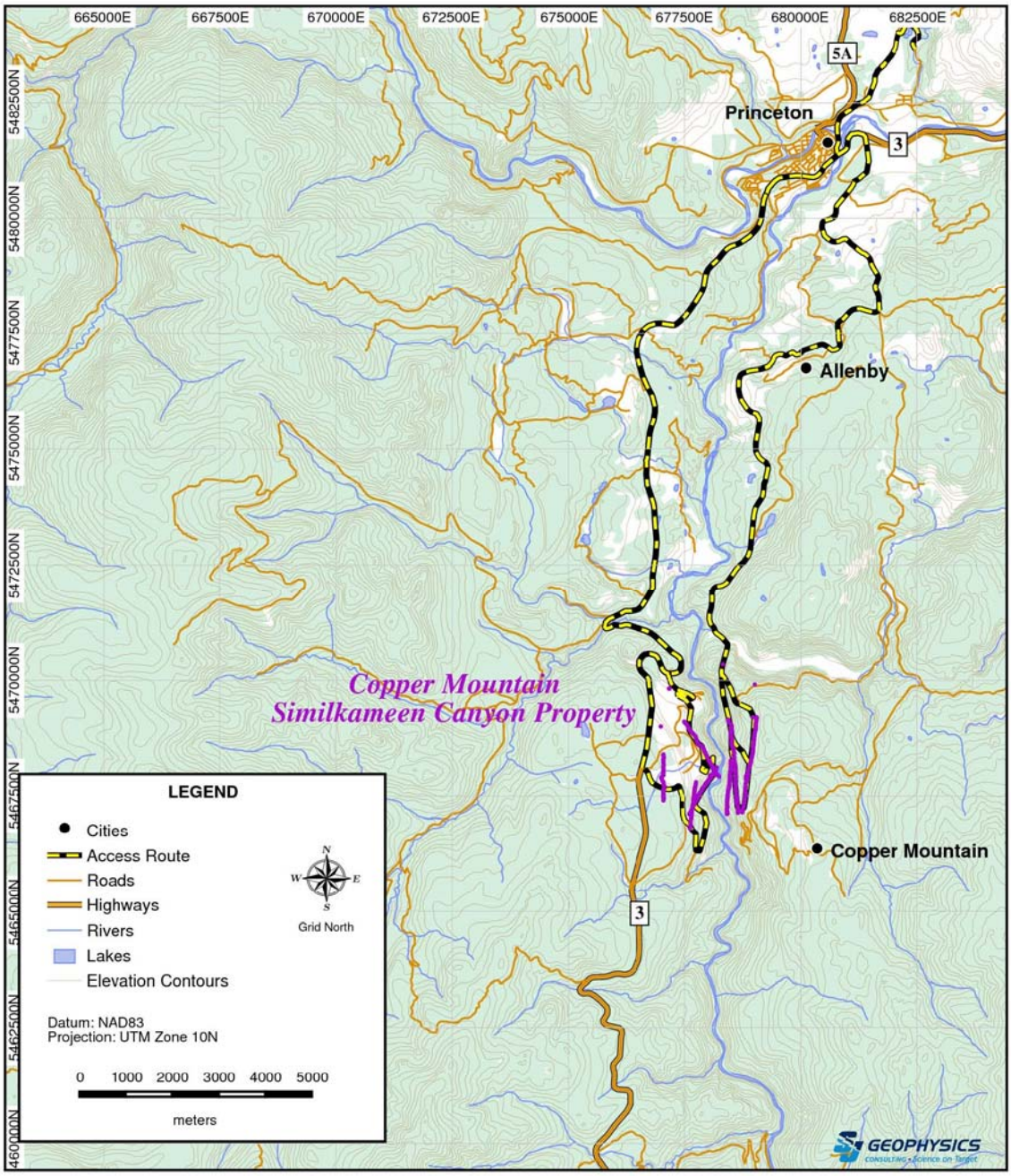

Figure 1.3*:* *Location of access roads and survey lines, Copper Mountain, Similkameen Canyon Project.*

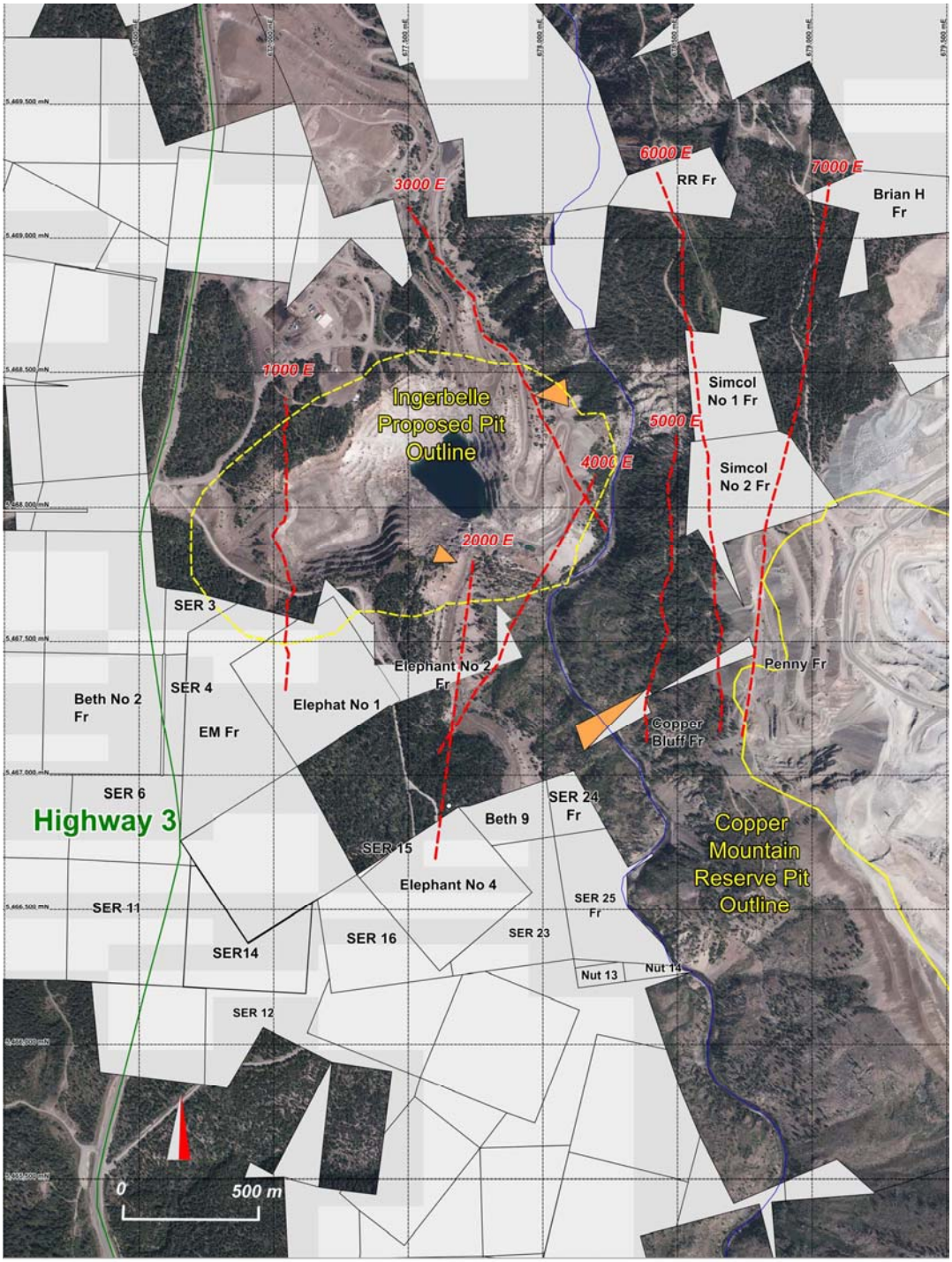

Figure 1.4: Plan view of geophysical survey lines with mineral claims (white). Actual distance of survey lines on mineral claims is 19% of the survey, but to obtain the full depth profile of the geophysical data on the claims, surveying needs to extend more than 200m beyond the claim boundary, thereby requiring 39% of the total survey distance.

2. Geology

2.1 Regional Geologic Setting

The Copper Mountain area is host to British Columbia's southernmost alkali porphyry deposits within Quesnel terrane (Fig. 2.), an extensive north trending, allochthonous belt comprised of the Nicola Group arc volcanic and related sedimentary rocks deposited on deformed Paleozoic arc volcanic and sedimentary rocks. The Quesnel terrane and a very similar northern equivalent, the Stikine terrane, are separated by the Cache Creek terrane, an oceanic accrectionary assemblage (Nelson and Colpron, in press). Amalgamation of these terranes, as well as the Yukon Tanana and Slide Mountain terranes to form the Intermontane Belt (or super terrane) began in the Late Paleozoic and was largely completed by mid-Jurassic time (Monger *et al*., 1992). Late Triassic to Early Jurassic calc-alkaline and alkaline porphyry deposits occur along the full extent of the Quesnel, Stikine and, arguably, the Yukon Tanana terrane (Nelson and Colpron, 2007) forming a mineralized trend nearly 1,800km in length.

Most of the southern part of the Quesnel terrane is formed by the Nicola Group rocks containing a thickness upwards of 7,000m of volcanic, sedimentary and coeval intrusive rocks of the Late Triassic age (Preto, 1972, 1979). The Nicola Group is predominately a mafic (basalt-andesite) volcanic assemblage of flows, breccias, epiclastic and pyroclastic rocks, derived sediments and locally, argillite and limestone. The volcanic rocks are characterized by being dark coloured, quartz saturated, but rarely quartz-bearing, clino-pyroxene (+/-plag) porphyrtic basalts, locally with analcime. The Nicola Group has been divided into four lithological assemblages/structural belts by Monger (*et al*., 1992, 1989) and Monger and McMillan (1989) which can be summarized as: 1) western belt – steeply dipping, east-facing, late Carnian to Norian, subaqueous felsic, intermediate and mafic calc-alkaline flows grading up into volcaniclastic rocks; 2) central belt – early to middle Norian, subaqueous to subaerial basalt and andesite flows, volcanic breccias, and lahars of both alkalic and calc-alkalic affinity; 3) overlying, westerly dipping, "eastern volcanic belt" (late Norian) composed of subaqueaous and subaerial, alkali, intermediate and mafic volcanic flow, fragmental and epiclastic rocks that were deposited on, or between, several well-defined emergent volcanic edifices; and 4) eastern sedimentary assemblage; (Ladinian to middle Norian) that is overlapped by the eastern volcanic belt and is composed (mostly) of greywackes, siltites, argillites, alkali intermediate tuffs and reefal limestone, possibly deposited in back-arc subaqueous environment. The Copper Mountain area is situated within the 'eastern volcanic belt' of the Nicola Group.

The Nicola Group hosts several, Late Triassic, alkalic intrusions, including the Iron Mask batholith and the Copper Mountain intrusions, as well as numerous smaller intrusions, most of which occur in the eastern volcanic belt. Intrusive compositions range from pyroxenite to syenite, although diorite and monzonite are the most common, and most are compositionally similar to their volcanic host rocks (Lang, 1993). Additionally, dykes, dyke swarms, and

intrusive breccias are common features, suggesting sub-volcanic intrusion. In contrast, the Late Triassic, calc-alkaline intrusions of the Quesnel terrane differ from the alkalic intrusions in that they tend to be larger, more compositionally homogeneous, and display less evidence of being sub-volcanic and occur in all four belts of the Nicola Group.

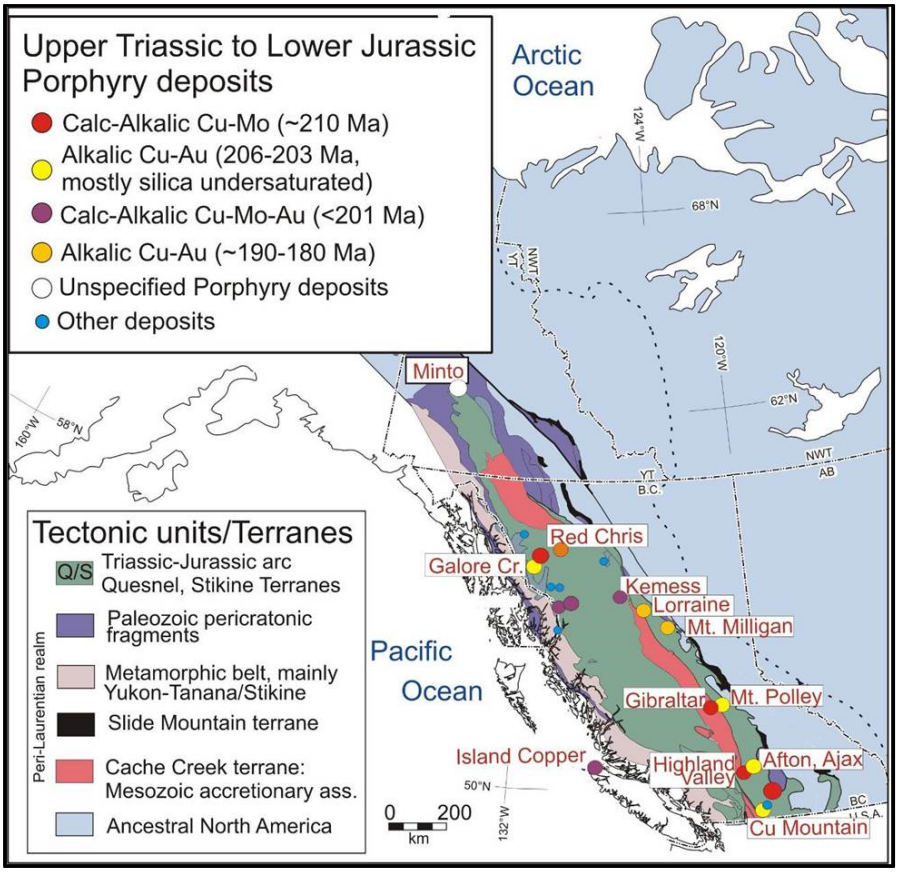

Figure 2.1: Tectonic Terrane Map of British Columbia with locations for Upper Triassic to Lower Jurassic porphyry deposits.

2.3 Property Geology

The geology of the Copper Mountain area is dominated by four rock units: the Nicola Group (eastern belt), the Copper Mountain stocks, the Lost Horse Intrusive complex, and the unconformably overlying, Tertiary, Princeton Group volcanic and sedimentary rocks (Fig. 3). The first three units are closely spaced in age and believed to be co-magmatic (Stanley *et al.*, 1995; Mihalynuk, *et al.* 2010) and similarities in both composition and texture, can make field identification difficult, particularly where the rock has been hydrothermally altered, and therefore, contacts should be considered generalized.

Initial bedrock exposure in the mine area was generally poor due to a moderately thick cover of glacial till, with the best exposures provided by the steep canyon walls of the Similkameen

River. Most of the current rock exposure in the mine area is from Pit walls, road cuts and drill core. The area of known mineralization is generally constrained by the Boundary Fault (Preto, 1972) on the western side, the Verde Creek pluton on the eastern side, and thick deposits of the Princeton Group to the north. Both the Copper Mountain Stock and Nicola Group volcanic rocks continue to the south, and although a considerable amount of exploration has taken place along the southern periphery of the stock over the years, no significant resources have been defined. Lost Horse intrusions appear to be absent in the southern area.

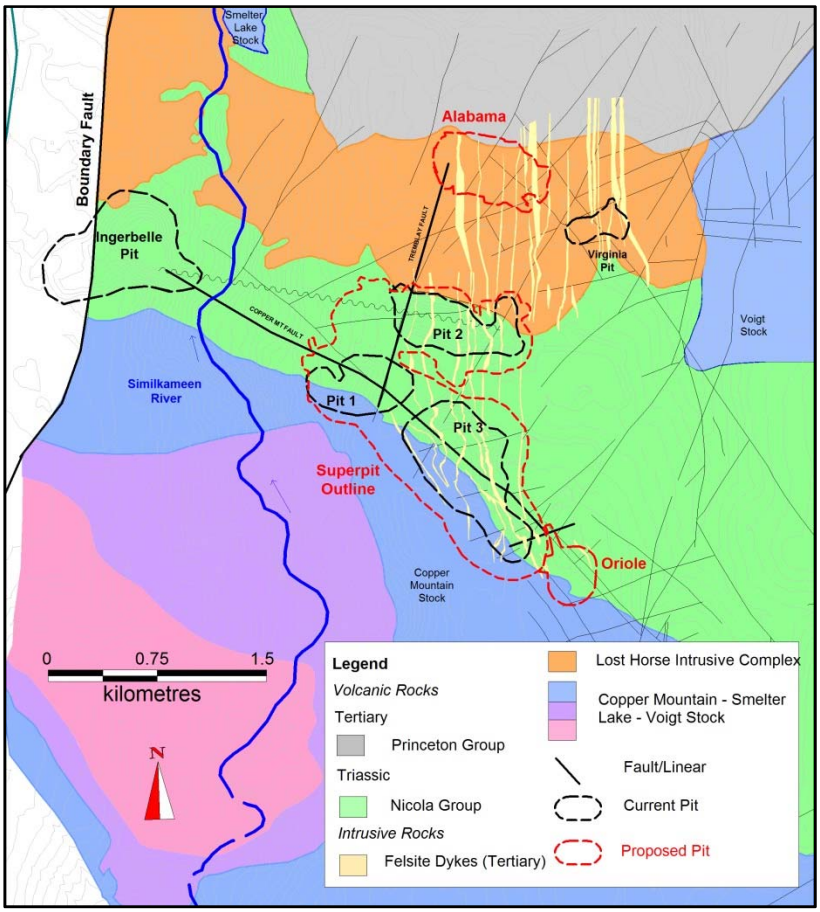

Figure 2.2: *Simplified property geology of the Copper Mountain area and displaying the relative locations of historical pits and current 'superpit'.*

2.3.1 Stratigraphy

A stratigraphic sequence of volcanic and sedimentary rocks has not been defined for the Nicola Group within the Copper Mountain area, however, the Group includes: 1) massive and rarely pillowed mafic and intermediate flows and flow breccia; 2) coarse volcanic breccia with rounded clasts (agglomerate), sometimes containing hornblende-phyric monzodiorite clasts; 3) felsic and intermediate water-lain tuff (greywacke) and lapilli-tuff; 4) volcanic siltstone, sandstone, conglomerate and minor limestone. These rocks are exposed in a northwesterly trending belt,

approximately 1,100 m wide and 4,300 m long, sandwiched between various intrusive phases (Figure 7.2). Bedding orientation is most commonly flat or at shallow angles, as based on correlation of units between drill holes and actual bedding structures within oriented core but is locally variable, suggesting some block faulting with rotation and/or possibly some minor folding.

Four predominant rock types are observed in the open pits and commonly form a major proportion of the economic mineralization. However, hydrothermal alteration and thermal contact effects from various intrusive phases obscures finer lithological details, and contact relationships between the units are often unclear or difficult to interpret. In decreasing order of abundance, the units are:

1) Coarse-grained agglomerates which are poorly sorted, sub-rounded and with varying abundance of clasts ranging from clast supported to matrix supported. Matrix is fine-grained, weakly porphyritic andesite, whereas clasts can be similar to the matrix, or consist of hornblende-phyric monzodiorite (commonly with aligned phenocrysts) and rare black mudstone. This unit is observed in all of the open pits.

2) Fine-grained, aphyric to sparsely plagioclase-porphyritic andesite flows of dark green to black colour. The plagioclase phenocrysts are zoned from calcic to sodic (rims). This unit is also observed in all of the pits.

3) Thinly bedded felsic tuffaceous epiclastic to sedimentary rocks. The most distinctive unit is a series of colour banded siliceous ash tuffs or chert.

4) Clast supported breccia with a medium grey mudstone matrix and clasts of sedimentary rocks from #3 above. This unit is interpreted to be a slump breccia and has only been observed in Pit 2 and the Virginia Pit, suggesting a limited depositional environment.

2.3.2 Intrusive Rocks

The Copper Mountain Stock (CMS) dominates the property in terms of size and exposure as seen in Figure 2.2 and 2.3. The stock is concentrically zoned from a diorite margin with local gabbroic zones, through monzonite to a syenite core. The core is non-magnetic (as illustrated by the airborne magnetic data image of Figure 7.3), leucocratic, and locally pegmatite-textured. The zonation is believed to indicate a normal fractionation process as opposed to multiple intrusions (Montgomery, 1968). The CMS does not host significant mineralization, although minor zones of copper sulphide minerals occur in the core area and within shear zones in the outer phases. The south wall of Pit 3 cuts into the outer margin of the CMS and here one can observe mineralized veins within the volcanic rocks extending for a few metres into the diorite before pinching out.

The Voigt and Smelter Lake stocks occur on the north edge of the Nicola Group volcanic rocks. These stocks are smaller than the CMS and do not exhibit any visible zonation, however, magnetic data indicate that the core of the Voigt Stock had lower magnetic susceptibility than the outer part, suggesting that it may be cryptically zoned. Both the Voigt and Smelter Lake stocks are petrologically similar to the diorite phase of the CMS, being equigranular, to sub-porphyritic, fine to medium grained monzodiorites

Immediately to the north of the Nicola Group rocks, is an area of dykes, sills and irregular plugs known as the Lost Horse Intrusive Complex (LHIC; Montgomery, 1968; Preto, 1972). The LHIC is a multi-phase suite of diorite, monzonite, and syenite which intrude the Nicola volcanic rocks, and are, for the most part, younger than the CMS, Smelter Lake and Voigt stocks, as indicated by cross-cutting relationships and the presence of monzodiorite clasts within dykes of the LHIC. Within the area mapped as LHIC (Figure 7.2) only about one half is actually intrusive, the rest being composed of screens and blocks of altered volcanic rocks, as indicated by exploration drilling in the Alabama area. The great variety of petrologically distinct intrusions which form the complex have been subdivided into four groups: LH1g, LH1b, LH2 and LH3 (Stanley, et al, 1996).

LH1 intrusions are pre-mineral and are similar to the Voigt stock but lack the poikilitic K-spar and biotite. LH2 intrusions range in composition from monzonite to syenite, although the later composition may actually be a product of alteration, are mineralized and typically display a strong alignment. LH3 intrusions are leucocratic, very fine-grained, monzonite to syenite in composition and cross-cut mineralization. To the northeast of the Copper Mountain camp is a large stock of calc-alkalic quartz-monzonite and granodiorite known as the Verde Creek stock. This stock is Cretaceous age and cuts the Voigt stock on its northern margin.

Geology of the Copper Mountain camp showing the known and inferred major structures within the camp is shown in Figure 7.4. The planned extents of operating open pits are outlined in black, whereas possible pit limits of mineralized zones are shown in blue, and other mineralized areas are shown in grey. The southernmost structure, the Copper Mountain fault is the most significant with the northeast trending structures being the next most significant in terms of controlling mineralization. Known and inferred structures appear to form a pattern of concentric and radially fractures about the Copper Mountain Stock.

The youngest intrusions in the camp occur as a series of north trending, vertical dykes of probable Eocene age. These dykes are most prominent in the eastern part of the camp and are well exposed in Pit 2 where a number cross the pit. The dykes are pale pink to yellow and consist of flow-banded, quartz-feldspar (+/- hornblende) porphyry ‘felsite.’ Dark green to black aphyric mafic dykes also occur but are subordinate to the felsic variety. Both types are interpreted to be feeders to Princeton Group volcanic rocks, that along with sedimentary rocks, filled extensional

grabens during Eocene time (Monger, et al., 1992). Princeton Group volcanic rocks overlie the LHIC on the north side of the Alabama zone.

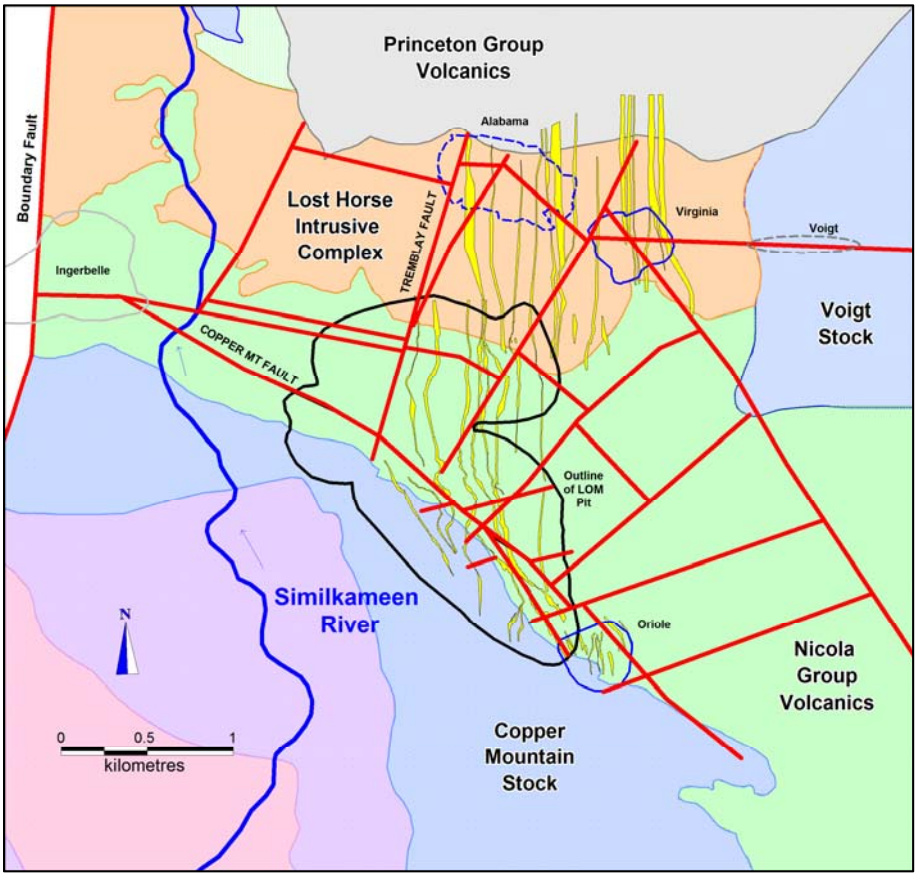

Figure 2.3: *Major Structures in the Copper Mountain Camp*

2.3.3 Structure

Structure, in the form of faults and fractures, has a great deal of significance to exploration as they control both the location of mineral deposits and the distribution of mineralization within the deposits. Although likely to be somewhat generalized, the faults and fractures that are related to mineralization appear to be concentric and radial fracture zones around the Copper Mountain Stock. Faults, along the north edge of the CMS (Copper Mtn. fault) and south edges of the LHIC and Voigt Stock, control the location of the Oriole prospect, Pit 1 and Pit 3 deposits, the Ingerbelle deposit and possibly the Pit 2 deposit. Another structure, crossing through the central area of the LHIC, hosts the narrow Voigt zone, the Virginia deposit, and the Alabama deposit. Within Pit 3, many of the vertical pipe-like "high-grade" zones (>1% copper) mined by underground methods are situated at the intersection of northeast trending faults with the Copper Mountain fault or adjacent sub-parallel structures. Within the deposits a high proportion of the

mineralization is controlled by multidirectional, but predominately vertical, fractures. The large faults controlling the major deposits are not simple breaks but should be considered to be wide zones of breakage with a multitude of intersecting fractures with a generally common orientation.

A study of surface fabric using Lidar data to indicate fault structures was carried out on the Similkameen River Canyon area. Results of this work are displayed in Figure 2.4 and appear to be complimentary to the geophysical data. However, suspected faults that appear to bound the Ingerbelle mineralization the northwest and northeast did not appear to be reflected in topography.

2.4 Mineralization

Mineralization at Copper Mountain is classified as an alkalic porphyry deposit(s). As a broad simplification, mineralization at Copper Mountain consists of structurally controlled, multi-directional veins, fracture fill, breccia zones and localized disseminations. Mineralization has been subdivided into four types, as follows: 1) veins, fracture fill and disseminated chalcopyrite, bornite, chalcocite and pyrite in altered Nicola and LHIC rocks; 2) hematite-magnetite-chalcopyrite replacements and/or veins; 3) bornite-chalcocite-chalcopyrite associated with pegmatite type veins and 4) magnetite breccias. Each mineralization type can be found in all pit areas, but each pit is unique with respect to the relative quantities and character of mineralization type. The alteration that is associated with each mineralization type has some degree of variation as well. Each pit area also has distinctive Cu:Ag:Au ratios (Table 2.1) which reflects the relative abundance of mineralization and alteration type, and possibly a zonation caused by a camp scale thermal regimes related to pre and syn-mineral intrusions.

Pit	*Tonnes*	*Cu%*	*Au g/t*	*Ag g/t*	*Au g/t*	*Ag g/t*
			Recovered grades		**Estimated head grades**	
Ingerbelle	58.5	0.43	0.171	0.703	0.244	1.326
Pit 2	30.0	0.38	0.089	0.754	0.127	1.423
Pit 3	45.0	0.46	0.069	1.890	0.099	3.566
Pit 1	15.0	0.48	0.055	1.210	0.079	2.283
Underground	31.5	~1.06	0.185	4.322		

Table 2.1: ***Tonnage and Grade of Historical Mining (1927-1996)***

A comparison of mined deposit grades and sizes is given in Table 2.1, and the data indicates the zonation northwards in decreasing silver and increasing gold from Pit3 through Pit1 to Pit 2 and Ingerbelle (data taken from Stanley et al. 1996). Copper grades are head grades, whereas precious metal grades in the first columns are recovered grades in concentrates and the second columns contain estimated head grades based on 'generalized' 70 and 53% recoveries for gold and silver, respectively.

Figure 2.4: Image of 1m contours from Lidar Survey, interpreted fault structures denoted by dashed lines.

Full size image below

Copper Mountain Mine
10m LiDar Contour
Similkameen Canyon River Area

Legend

- Fault
- Thrust Fault
- Suggested Fault
- Lake
- River
- Road

250 0 250 500 750 m

Pit 3 was excavated in the area of the Granby underground workings and hosted the largest amount of mineralization. Descriptions of this mineralization (Fahrni, 1951) combined with underground stope plans indicate that much of the underground mineralization occurred as tabular to pipe-like zones of veining and breccias controlled by faults and fault intersections. Dimensions of subsidence zones above the underground workings were approximately 100-180 m in diameter, near surface, with vertical extents of approximately 350m. Originally referred to as "bornite ore", remnants of this material found in collapsed material while open-pit mining were observed to contain considerable quantities of hypogene chalcocite. Veins, veinlets and disseminated sulphide mineralization surrounded the breccia cones and provided most of the mineralization subsequently mined from the open-pit.

In contrast to Pit 3, the Ingerbelle deposit had chalcopyrite as the dominant copper species and contained more disseminated mineralization. The Ingerbelle deposit is somewhat centered on the intersection of at least two major structures, both of which appear to contain some massive to semi-massive sulphide veins at depth (as indicated by both historical drill holes and more recent exploration drilling in 1994). Geologically, the Ingerbelle pit area is significantly complex, being cut by three phases of dykes, two of which are associated with mineralization. Alteration consists of both albitic and potassic metasomatism and later (?) multi-stage sulphide +/- K-spar and/or albite veining. A significant magnetite breccia body, since mined out, occurred within the Ingerbelle Pit area and remnant pieces indicate angular to rounded, potassically altered fragments supported in a magnetite matrix. Dyke-like appendages of the magnetite breccia are locally visible in the pit walls. Scapolite fills many late stage fractures which can be observed in the southern wall of the pit.

The Virginia deposit is formed by two parallel, west-northwesterly trending magnetite sulphide veins of 3 to 7 m in thickness. The veins are sub-continuous and surrounded by disseminated and fracture controlled chalcopyrite in potassically altered volcanic, sedimentary rocks of the Nicola Group, and intrusive rocks of the LHIC. Along the strike of the veins, approximately 1.6km to the east is the Voigt zone where historical drilling (circa 1920- 1950's, and 1987) intersected grades between 0.5 and 1.5 g/t gold and 0.5 to 1.5% copper over a single, magnetite (+/- hemetite) rich vein-type structure with variable widths between 5 and 15m. The Voigt zone is hosted entirely within diorite of the Voigt Stock. The vein-stock contacts are sharp with only minor epidote veining within the stock as alteration.

The Pit 2 area is similar to the Ingerbelle pit in geological complexity. A more pronounced structural control is evident with chalcopyrite mineralization occurring in east and northeast trending veins, vein stockworks and fracture fillings. Some disseminated mineralization is present peripheral to syenite dykes of the LHIC and in a magnetite breccia that occupied the north central part of the pit area.

A large variety of alteration types, commonly overlapping, occur throughout the Copper Mountain Camp. Alteration can be classified according to its occurrence: either pervasive or structurally controlled, and its predominant mineral assemblage. The typical alteration assemblages associated with porphyry copper models (e.g.: Lowell and Guilbert, 1970) propylitic, phyllic, argillic, advanced argillic and potassic, and their zonal or spatial organization around a central intrusion are not present at Copper Mountain.

The earliest alteration assemblage at Copper Mountain is a hornfels produced within the volcanic rocks adjacent to the Copper Mountain Stock. The hornfels appears to affect only the intermediate to mafic volcanic flows and pyroclastic rocks while the sedimentary rocks are relatively unscathed. The hornfels is a dark purple-gray to black, hard, very fine-grained assemblage of diopside or biotite, plagioclase and magnetite, +/- other opaque oxide minerals (Preto, 1972). Volcanic fragments and matrix commonly react slightly differently to the hornfelsing event resulting in visually enhanced fragmental textures in some locations and virtually obscuring primary textures in other locations. The hornfelsed rocks seldom occur more than 700 m beyond the margin of the CMS. A spatial relationship between mineralization a hornfelsing was proposed by Farhni (1951), who suggested that the increased brittleness of the hornfels was more susceptible to fracturing and mineralization. Alternatively, or coincidently, it may be that the fine-grained magnetite of the hornfels was quite reactive with the mineralizing fluids providing an iron source to form sulphide minerals.

Sodium metasomatism, or pervasive albitic alteration, appears to be pre-mineralization and occurs as a pervasive albite-epidote hornfels. In addition to albitization of feldspars and conversion of ferro-magnesium minerals to epidote (+/- diopside and chlorite), magnetite and opaque minerals are destroyed. This process results in ‘bleaching’ of the original rock and reduction in grain size, forming a pale gray or greenish gray, very competent rock with complete destruction of primary textures. Indeed, much of the rock affected by Na-metasomatism was originally mapped as intrusive due to its fine-grained leucocratic appearance. However, detailed mapping within the open-pits indicates that Na-metasomatism affects all rock types to varying degrees. Trace amounts of pyrite maybe present within this alteration. Na-metasomatism is most pronounced along, and to the northeast of the Copper Mountain fault, and adjacent, or peripheral to, the hornfelsed rocks.

Pervasive potassium alteration is extensive throughout the district but tends to be outbound (northeast) of the previous alteration types, although it may locally overlap or crosscut both pervasive sodic alteration and hornfels. Potassic alteration replaces primary plagioclase with potassium feldspar and replaces ferro-magnesium minerals with biotite, epidote, calcite, chlorite and magnetite; typically producing rocks with a moderate to strong orange to pink colouration. Destruction of primary lithological textures occurs where the alteration is intense. Potassic alteration appears to be partly an outward zonation to the previous alteration types as well as

being spatially associated with certain phases (LH2) of the Lost Horse Intrusive complex (LHIC). Potassic alteration is temporally related to sulphide mineralization.

Numerous veins, vein envelopes and fracture-filling mineral assemblages and textures cross-cut, or occur within the pervasive alteration types (these vein types are listed in detail in Stanley et al. (1985)) but the more prominent ones are described below.

Magnetite veins: with or without copper sulphide minerals, of variable size from fine fracture filling to vein stockworks to sheeted vein swarms to 3-4m thick veins. These veins are not abundant in Pit 3 area but are significant in Pit 2 and comprise much of the ore within areas north of Pit2 and east of Ingerbelle.
"Pegmatite veins": coarse grained potassium feldspar, biotite, epidote and calcite (+/- albite, apatite, garnet, and quartz) these veins are distinctive and occur with, or without, sulphide minerals. The veins are of variable size (up to 2 m thick), of variable orientation, and occur in dilatant zones throughout the camp.
Potassium feldspar veins: these veins range in thickness from 1 mm to 1 m and are generally barren; filling fractures within dilatant zones across the camp.
Chlorite veins: these veins are fine, 1-10mm, discontinuous, late and occur throughout the camp.

Figure 9.1 represents a schematic cross-section model of mineralization at Copper Mountain showing the relationships of the intrusions, structures and possible flow paths for hydrothermal fluids.

Late stage scapolite fracture filling is common in the Ingerbelle deposit but is rare elsewhere in the Copper Mountain area. The presence of the "pegmatite veins" and local calc-silicate alteration assemblages can give local areas the appearance of skarn formation; however, the initial calcic minerals are themselves an alteration product and no carbonate rocks have been recognized within the local stratigraphy.

In general, there has only been limited oxidation of the copper minerals at Copper Mountain, noticeably concentrated along the edges of the Lost Horst Gulch, which impacts the upper part of the Virginia deposit and the northern edge of the Pit 2 area.

3. Geophysical Program

3.1 Introduction

Copper Mountain Mine (BC) Ltd. ("CMML") engaged SJ Geophysics to undertake a 2D and 3D geophysical survey in the Similkameen canyon between current mining areas and historical mining areas on opposite sides of the Similkameen River.

3.1.1 Geophysical Techniques IP Method

The time domain IP technique energizes the ground by injecting square wave current pulses via a pair of current electrodes. During current injection, the apparent (bulk) resistivity of the ground is calculated from the measured primary voltage and the input current. Following current injection, a time decaying voltage is also measured at the receiver electrodes. This IP effect measures the amount of polarizable (or "chargeable") particles in the subsurface rock.

Under ideal circumstances, high chargeability corresponds to disseminated metallic sulfides. Unfortunately, IP responses are rarely uniquely interpretable, as other rock materials are also chargeable, such as some graphitic rocks, clays, and some metamorphic rocks (e.g., serpentinite). Therefore, it is prudent from a geological perspective to incorporate other data sets to assist in interpretation.

IP and resistivity measurements are generally considered repeatable to within about 5%. However, changing field conditions, such as variable water content or electrode contact, reduce the overall repeatability. These measurements are influenced to a large degree by the rock materials near the surface or, more precisely, near the measurement electrodes. In the past, interpretation of a traditional IP pseudosection was often uncertain because strong responses located near the surface could mask a weaker one at depth. Geophysical inversion techniques help to overcome this uncertainty.

3.1.2 Volterra-3DIP Method

Three dimensional IP surveys are designed to take advantage of recent advances in 3D inversion techniques. Unlike conventional 2DIP, the electrode arrays in 3DIP are not restricted to an in-line geometry. This means that data can be collected from a large variety of azimuths simultaneously leading to a highly sampled dataset containing more information about the Earth's physical properties. In an ideal world, a 3DIP survey would consist of randomly located current injections and receiver dipoles with random azimuths. Unfortunately, logistical considerations usually prohibit a completely randomized approach.

The Volterra-3DIP distributed acquisition system is based on state-of-the-art 4-channel, full-waveform, 32-bit Volterra acquisition units. The system is highly flexible and can utilize any number of Volterra units. The Volterra-3DIP system's untethered, distributed design, eliminates the need for specialized receiver cables and a centralized receiver control station. The dipoles can be in any orientation, can have varying lengths, and completely avoid inaccessible areas if necessary.

A typical Volterra-3DIP configuration establishes alternating current and receiver lines in sets of 5, but can be customized based on the project. The current lines are located on adjacent lines to the receiver line and current injections are performed sequentially at fixed increments (25m, 50m, 100m, 200m) along each current line. By injecting current at multiple locations along each current line, the data acquisition rates are significantly improved over conventional surveys. Customized receiver arrays are utilized to provide greater cross-line focus for a better azimuthal distribution of the data. Cross-dipoles are frequently used to maximize signal coupling and improve the surface resolution.

3.3 Survey Grid

The proposed survey grid consisted of seven lines. In general, these lines were set to follow existing roads and topographical benches; therefore, not all lines were straight. The survey crew altered the lines after seeing the terrain first-hand. Lines were straightened to provide data that would improve the 2D modeling process. The lines on the west side of the river (1000E, 2000E, 3000E, 4000E) were surveyed with the 2D technique. When acquiring data on the east of side of the river, in addition to acquiring 2D data, offset current injections were utilized on adjacent lines to allow the collection of some 3D data.

Line 1000E was surveyed as proposed except for some small adjustments around steep sections in the old open-pit mine. Line 2000E was straightened along a slightly different azimuth. Line 3000E was straightened substantially. Line 4000E was surveyed last and was positioned to join the gap between lines 2000E and 3000E. Line 5000E was surveyed with current injections along lines 5000E and 6000E. Line 6000E was surveyed with transmitter stations along lines 6000E and 7000E. Line 7000E was altered from its proposed version, with the line azimuth being adjusted to shift the southern end westward to avoid the mining operations occurring in the area. Line 7000E was surveyed with current injection stations along lines 7000E and 6000E.

All survey lines were planned with 25m stations. A pre-surveyed grid with flagging or stakes did not exist. The stations were navigated to based on way points up loaded to the crews' hand-held GPS units. The survey grid parameters are summarized in Table 3.1 and displayed in Figures 3.1 and 3.2.

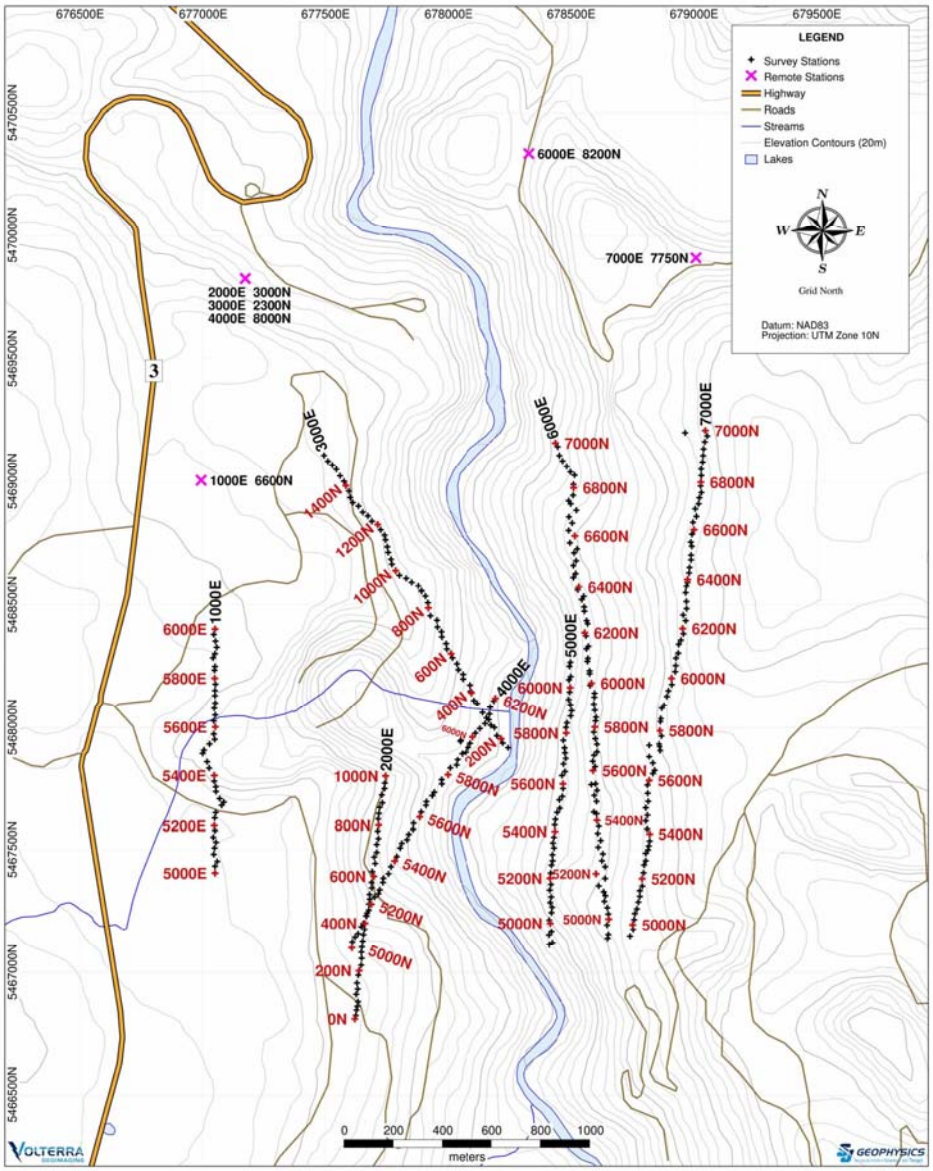

Figure 3.1: *Geophysical Survey Grid (actual) plotted on topography*

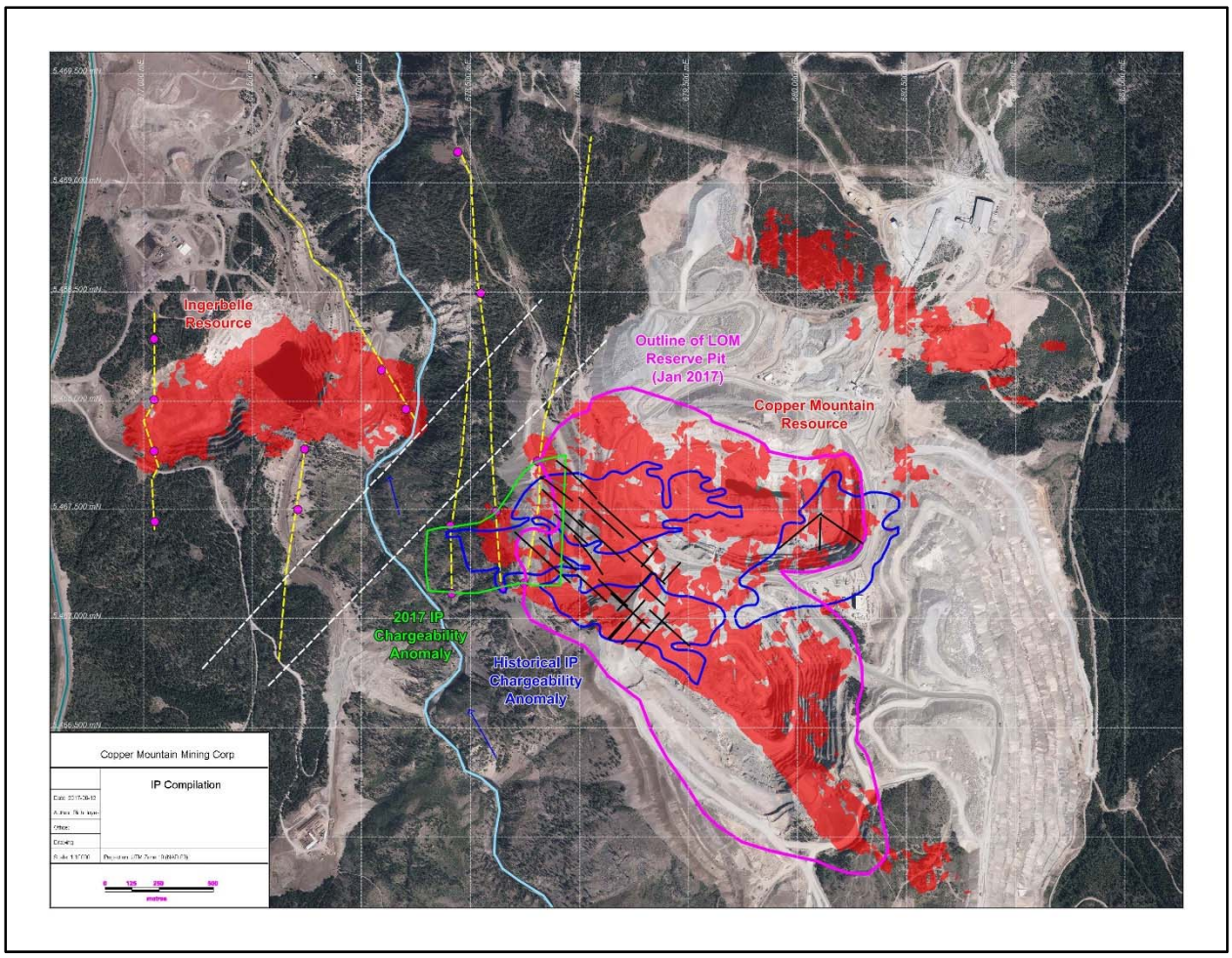

Figure 3.2: *Geophysical Survey lines (yellow) on an air-photo showing pit outlines, resource blocks >0.2% Cu (red), historical IP chargeability highs (blue), and possible fault structures (dashed white).*

3.4 Survey Parameters and Instrumentation

3.4.1 Volterra Distributed Acquisition System

The Volterra Distributed Acquisition System was developed internally by SJ Geophysics. The heart of the system are the Volterra data acquisition units, internally known as Dabtubes. Each four-channel Volterra acquisition unit contains 24-bit analog-to-digital electronics that record the full waveform signal from various sensor configurations. This allows for varying suites of geophysical techniques such as IP, electromagnetics (EM), magnetotellurics (MT), controlled source audio-frequency magnetotellurics (CSAMT), etc. to be measured. The recorded full-waveform data is then

passed through proprietary signal processing software to calculate the relevant geophysical attributes (ie. apparent resistivity/chargeability for IP surveys).

3.4.2 Volterra-2D/3DIP Survey

SJ Geophysics Ltd.'s proprietary Volterra Distributed Acquisition System was utilized for the IP survey. Current injections were controlled using a GDD TxII transmitter and the resulting ground response was measured using each Volterra data acquisition unit.
The distributed nature of the Volterra-3DIP system allows for highly customizable array and survey configurations. The resulting flexibility is a huge benefit in challenging terrain conditions where rivers, roads, cliffs, or other obstacles can easily be avoided. The crew took full advantage of these features to optimize the field logistics and maximize production.
The transmitter and IP signal recording/processing parameters used for the survey are described in Table 3.1. The full instrument specifications are listed in Appendix II.

IP Transmitter	GDD TxII
Duty Cycle	50%
Waveform	Square
Cycle and Period	2s on / 2s off: 8s
IP Signal Recording	Volterra Acquisition Unit
Reading Length	120s
IP Signal Processing	CSProc (SJ Geophysics proprietary software)
Vp Delay, Vp Integration	1200ms, 600ms
Mx Delay, # of Windows Width (Window Width)	50 ms, 26, 28, 30, 32, 34, 36, 39, 42, 45, 48, 52, 56 60, 65, 70, 75, 81, 87, 94, 101, 118, 128, 140, 154, 150 (50-1950ms)
Mx Integration (Inversion)	50-1950ms (Windows 1-26)
Properties Calculated	Vp, Mx, Sp, Apparent Resistivity and Chargeability

Table 3.1: 2D and 3D IP Transmitter and reading parameters

Receiver dipoles were set up using 50cm long and 1cm diameter stainless steel electrodes hammered into the ground and connected into the array by double conductor wire. The electrodes used for current injections were significantly larger at 1m x 1.5cm with two electrodes used at each injection site to improve ground contact. Current electrodes were connected to the current transmitter by a single conductor wire.

The Volterra-2D & 3D IP system was configured using a combination of in-line and interlaced in-line arrays. Lines 1000E-3000E were surveyed with interlaced in-line arrays, and Lines 4000E-7000E were surveyed with standard in-line arrays. Details of the survey configuration are described in Table 3.2. Schematic representations are presented in Figures 3.3 and 3.4.

2D Acquisition Set	1 Line: (Tx/Rc)
3D Acquisition Set	2 Lines : (Tx-Tx/Rc)
Active Array Length per Reciever	Minimum 1000 Maximum 2075
Total Active Dipoles per Current Injection	Min 26 – Max 41
Dipole Length	50m & 100m
Current Interval	50m

Table 3.2 Volterra-2D & 3D IP Survey Parameters

For the interlaced array, dipoles were set up along the receiver lines in clusters of four, with interlaced dipoles of lengths ranging from x_1= 100m to x_2= 50m. Adjacent clusters share a common electrode at either end. The interlaced cluster approach takes advantage of the four available channels, improves data quality, and provides data redundancy in the event that data from one dipole is lost.

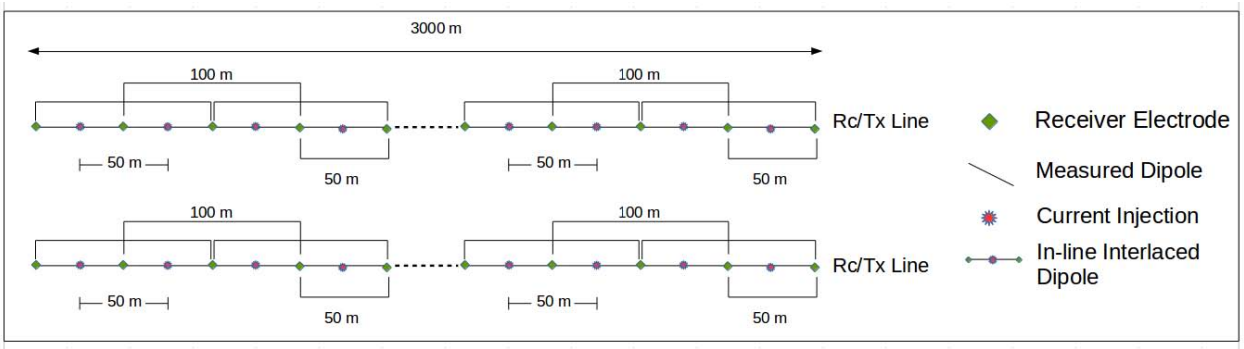

Figure 3.3: Schematic representation of the Interlaced in-line array

The decision was made half-way through the project to switch the array configuration to a standard, in-line 2D-array. The interlaced array added complexity that was deemed unnecessary.

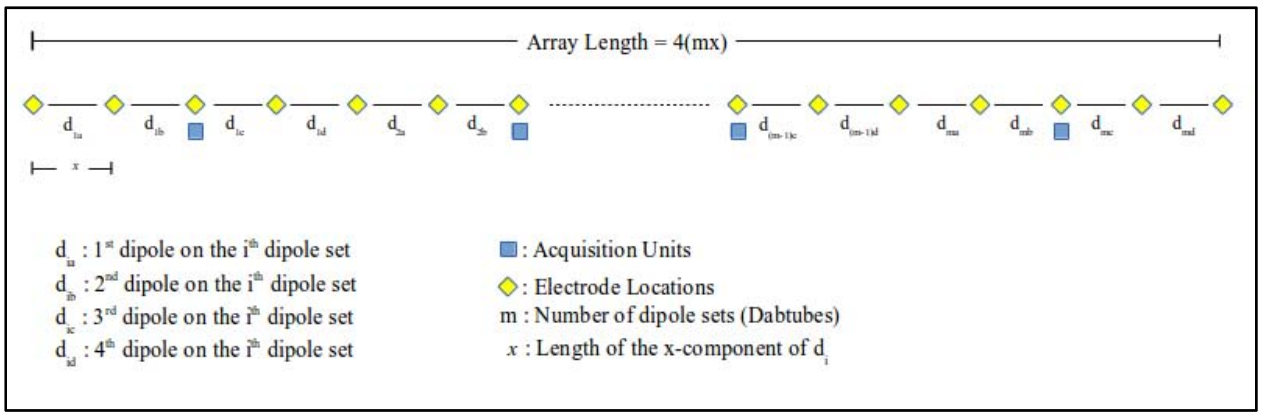

Figure 3.4: Schematic representation of the in-line array.

A total of 4 different remote electrode stations were utilized over the course of the survey. The locations of the remote current electrodes are listed in Table 5 below.

Name	Label	Easting	Northing
North Remote	1000E 6600N	676994	5469005
North Remote 2	2000E 3000N 3000E 2300N 4000E 8000N	677173	5469824
North Remote 3	6000E 8200N	678329	5470336
Norte Remote 4	7000E 7750N	679010	5469908

Table 3.3: Location of 3DIP remote sites (WGS84 Z10)

All location information was recorded using hand-held GPS units. The crew used Garmin GPSMAP 64s and 62s model devices, collecting waypoints at all receiver electrodes and current injection sites.

3.5 Field Logistics

The SJ Geophysics field crew consisted of 3 field geophysicists and 2 technicians to perform the day-to-day operations of the survey. This team oversaw all operational aspects including field logistics, data acquisition, and initial field data quality control. Table 3.4 lists the SJ Geophysics crew members on this project. SJ Geophysics crew's first day on the Copper Mountain Similkameen Canyon project was May 30th and they remained on site through to June 8th. Mobilization to the project occurred on May 30th and demobilization from the project site to Kamloops was on June 9th.

Crew Member Name	Role	Dates on Site
Jordan Perk	Field Geophysicist	May 30 – June 8
Nathan Anderson	Field Geophysicist	May 30 – June 8
Jay Enns	Field Geophysicist	May 30 – June 8
George Jordan	Field Technician	May 30 – June 8
Jeff Moorcroft	Field Technician	May 30 – June 8

Table 3.4: SJ Geophysics Crew members.

During the geophysical survey, SJ Geophysics conducted safety meetings in the form of daily "tailgate meetings". At the tailgate meetings, personnel discussed issues related to weather conditions (including ramifications on the survey/personal safety), encounters with or sightings of potentially problematic wildlife, efficient organization of daily tasks, and any other work-related questions or concerns. On June 1st, the crew participated in a mine site safety orientation at the Copper Mountain administration building on the mine site.

The SJ Geophysics crew was accommodated at the Princeton Castle Resort, in Princeton, BC. The accommodation consisted of a large house complete with kitchen, quality WiFi, and a nice deck. Two vehicles supplied by SJ Geophysics were utilized for the project. The drive to the survey area took approximately 30 minutes each way from the accommodation site to reach either the east or the west side of the project. To drive from the east side of the project to the west took approximately 40 minutes, however, this was only required on two of the days. All access roads to the project site were gated and locked. Keys were provided by the client representative. The survey progressed from west to east. The crew started in the west at Line 1000E. Line 1000E had easy access and was relatively simple in terms of logistics. This allowed the crew some time to plan future lines.

Each acquisition day began with the setup of the Volterra acquisition units along the receiver lines and the setup of the transmitter site. If necessary, breaks in the wire linking the remote station to the transmitter were fixed.

Breaks in the wires were frequently caused by roaming wildlife each night and were often difficult to find, especially along the transmitter lines. Locating and fixing these breaks regularly was unavoidable and time consuming. Prior to field data acquisition, a contact resistivity test was performed using a small waveform generator attached in parallel to each Volterra acquisition channel. This was done for each dipole in the array, and allowed the operator to identify breaks in the wire or areas of poor ground contact which could degrade input signal quality. Furthermore, this test allowed the operator to inspect the raw signal, ensuring that the Volterra acquisition units were functioning correctly, and to ensure that the receiver was synchronizing with the correct GPS time.
Upon completion of these tasks, acquisition would begin. During acquisition stages, a dedicated 'transmitter' Volterra acquisition unit and a current monitor were used to measure the current being injected at each station. By inspecting the quality of the current output, the transmitter operator can detect current leakage and ensure the transmitter is functioning correctly. An Android tablet with proprietary Volterra software was used to record the current injection start time and duration as well

as to visually check the output signal. After equipment set-up was complete, data acquisition required only three crew members, leaving two members to begin wire set-up on the next line to be surveyed. As most lines needed some modifications from the original design, this task began with a thorough reconnaissance of the survey area. Once the plan was formulated, the line was prepared. The lines were created somewhat 'on the fly' in the field. An assortment of field techniques were employed to achieve this, all of them depending heavily on the hand-held GPS units carried by the field personnel. The general technique involved identifying and sharing anchor points. These points were chosen on account of bends in roads, talus slopes, or similar physical considerations. The crew members would begin at one end of a new line and navigate between the anchor points, moving sequentially in 50m intervals measured by the GPS units. The results were exceptionally straight lines that used railroad benches and roads as much as possible.

At the end of every day, all electronic equipment was collected and brought back to the crew house to have the data processed and batteries charged.

The terrain in the survey area was steep. The crew took care while navigating the steep slopes and no incidents were reported. A variety of wildlife was encountered during the survey, including elk and bear. Tick levels were extreme. Crew members found multiple ticks daily. Thorough checks were done every evening and only one actual bite was discovered.

3.6 Field Data Processing & Quality Assurance Procedures

3.6.1 Locations

Good quality location data is the first step to the successful analysis and interpretation of geophysical survey data. Garmin GPSMAP 62s and 64s handheld GPS units were utilized to collect location information. Measurements are taken at every survey station where satellite reception was acceptable. The quality of the location data and labeling were checked every night using GPS management software such as Garmin BaseCamp or GIS packages like QGIS and GRASS. Any inconsistent measurements were discarded and the remaining points, referred to as control points, were incorporated into a database using proprietary software called Location Manager. Any missing or discarded survey station locations were re-acquired the following day.

GPS measurements typically have a much lower accuracy in the vertical direction compared to the horizontal direction. A quality digital elevation model (DEM) was provided by the client (2m and 5m) for the survey area. The GPS elevation data was replaced with the more ccurate DEM elevations.

3.6.2 Volterra-2D/3DIP Data

The Volterra-IP data went through a series of quality assurance checks, both in the field and in the office, to ensure that the data was of good quality. At the end of each acquisition day the recorded signal was downloaded from the Volterra acquisition units to a personal computer. The signals were

then clipped to the GPS time windows of each current injection, lightly filtered for noise, and imported into SJ Geophysics' proprietary QA/QC software package called JavIP. This software package integrates location data with DCIP data in order to calculate the apparent resistivity and apparent chargeability values. JavIP contains interactive quality control tools to allow the field geophysicist to display decay curves, view a dot plot of the calculated parameters, and manually reject bad data points.

The majority of the data points flagged for removal were due to null-coupling, a phenomenon typical in IP surveys related to the survey configuration. Null-coupling occurs when a receiver dipole is sub-parallel to lines of constant potential, leading to a significant decrease in signal strength and corresponding poor data quality. Additional data can also be deemed untrustworthy due to low signal quality or dipoles being inadvertently disconnected (usually due to animal activity).

After the first data quality review in the field, the database was delivered to SJ Geophysics' head office for a second review. The data were then carefully checked to ensure that erroneous data points had been removed and were not passed along to the final stage of processing: the inversion. Interpreted 3D models of the direct current (DC) resistivity and induced polarization (IP) were carried out utilizing UBC-Geophysical Inversion Facility (UBC-GIF) DCIP3D inversion algorithms.

3.7 Data Quality

3.7.1 Locations

In general, the GPS data quality were good over the entire area. Tree cover was predominantly sparse resulting in GPS accuracies that were commonly within 3m. Some areas of steep topography and heavy tree cover had accuracies degrade to near 7m.

3.7.2 Volterra-2DIP data

The 2DIP data collected during the Similkameen Canyon project was of good quality. Surface contact resistances were quite low in general but exceptionally low given the rocky nature of the surface layer.

Voltage potentials ranged from below 1mV to values greater than 5000mV. Readings with voltages over 5000mV are not be used as this is outside the range of the recording equipment. This only occurred in a few instances for dipoles that were very near the current injection site. On average, the voltage potentials were near 5mV. Apparent resistivity values were consistent and resulted in pleasing data trends.

It is believed the large ore conveying structure that crossed lines 6000E and 7000E may have corrupted a small, localized group of data. There is strong evidence in the observed data that the

structure was able to channel electric current, resulting in suspect data.

Measured voltages were strong and a strong background chargeability resulted in clean decay curves throughout the project. Chargeability measurements were very clean across the entirety of the IP lines. Dipoles that were at maximum offset recorded relatively low noise data.

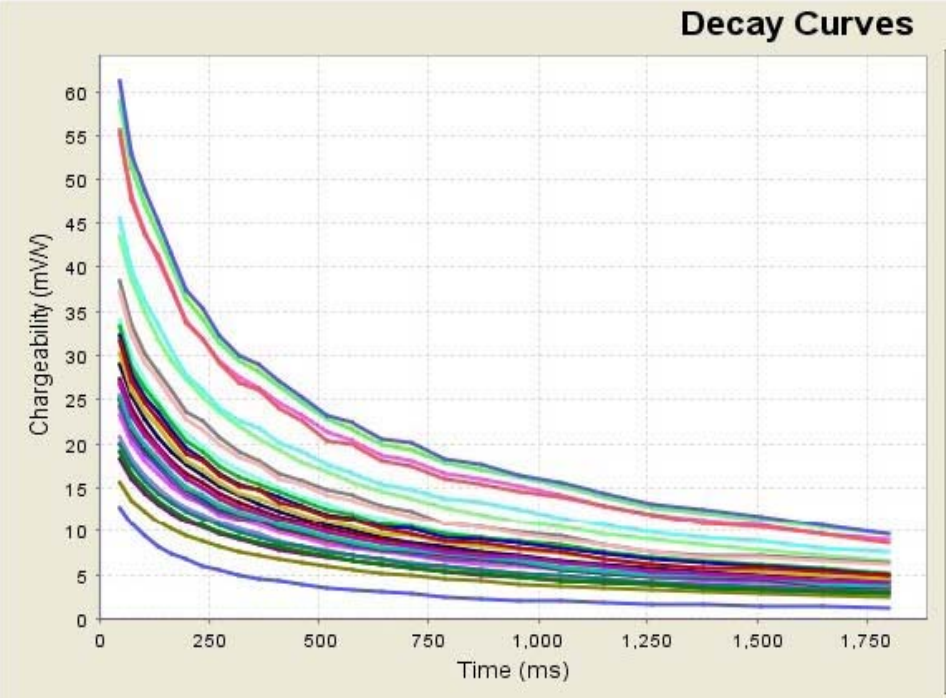

Figure 3.5: Example of clean decay curve. Line 3000E Station 1375.

Figure 3.5 shows data generated with a transmission current above 2A, and Figure 3.6 shows data generated with a transmission current below 300mA.

3.8 Geophysical Inversion

The purpose of geophysical inversion is to estimate the 3D distribution of subsurface physical properties (density, resistivity, chargeability, and magnetic susceptibility) from a series of geophysical measurements collected at the surface. Unfortunately, this is a challenging problem – the subsurface distribution of physical properties is complex and only a finite number of measurements can be collected. These complications lead to an under-determined problem. As a result, there are many different possible 3D physical property models that can be obtained which mathematically fit the observed data. Utilizing known geological and geophysical information to evaluate the model

allows the best or most geologically realistic model to be selected and leads to a better understanding of the subsurface.

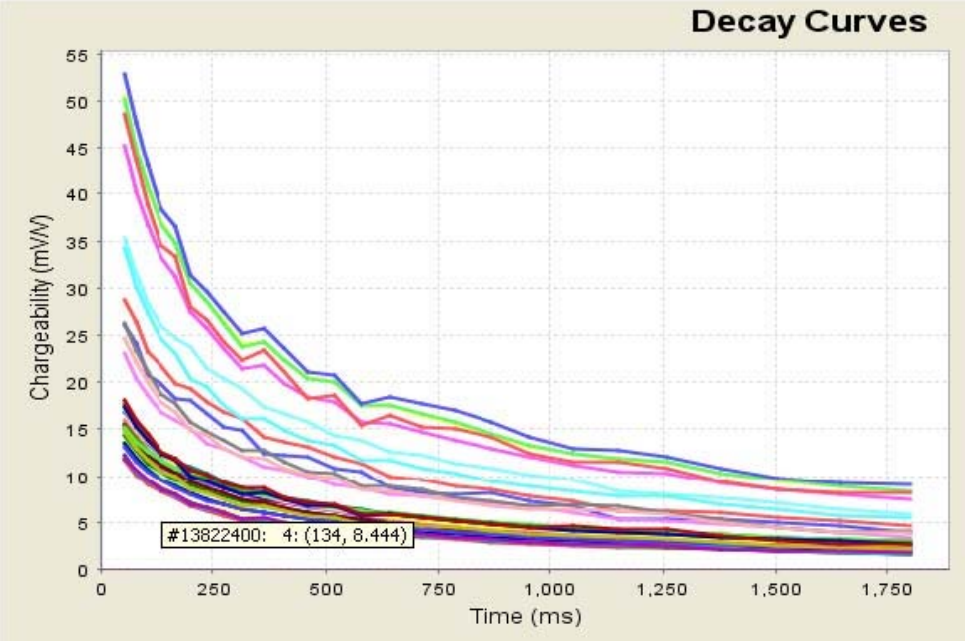

Figure 3.6: Example of relatively noisy decay curve. Line 3000E, Station 975

Geophysical inversions are commonly performed for every survey carried out by SJ Geophysics. Several inversion programs are available, but SJ Geophysics primarily uses the UBC-GIF algorithms (e.g. DCIP2D, DCIP3D, MAG3D, GRAV3D) which were developed by a consortium of major mining companies under the auspices of the University of British Columbia's Geophysical Inversion Facility.

In general, multiple inversions are carried out for each dataset and the resultant inversion models are compared with known information to evaluate the model. For example, known geology, drill assays, the estimated depth of investigation, and the quality of the input data are all used during the evaluation. The most geologically reasonable model that fits the data is then chosen as the best model. When available, additional information such as geological boundaries and down-hole geophysical data can be incorporated into the inversion in order to constrain the inversion model.

Once the final inversion model is selected, the model is gridded and mapped for interpretation. Typically, cross-sections and plan maps are created, sliced at different depths beneath the surface. The inversion results can be visualized in 3D using open source software packages such as Mayavi and Paraview in both 2D and 3D views. Additional data can then be overlain to aid in interpretation

and help facilitate the identification of potential drilling targets.

4 Results

Geophysical results are displayed on a series of pseudo sections and 2-D inversion sections for each line in Appendix III. 3-D inversion of both chargeability and resistivity data are presented as plan views of a rectangular area containing all the IP lines, at various depth slices in 50 to 100m depth increments, and is also presented in Appendix III.

4.1 Inversion Sections

Line 1000E: The inverted section shows two moderate to intense chargeability anomalies separated by an approximately 300m wide band of low chargeability material dipping to the south at approximately 30 degrees. The southern chargeability zone suggests that there may be a southward continuation of mineralization in the western lobe of the Ingerbelle pit, whereas the northern anomaly is well outside of the mineralized area but does fall on the northwest trend of mineralization extending all along Pit 3, Pit 1 and through Ingerbelle and therefore is somewhat intriguing. Resistivity data is vague, but does confirm a southerly dipping tabular aspect. 3-D resistivity data suggests that Line 1000E is outside of the altered and mineralized area, however the gap between 1000E and the adjacent lines may be just too large to form a respectable interpretation.

Line 2000E: This northern part of this line follows the old highway 3, which ran overtop of the Ingerbelle deposit, from the south edge of the Ingerbelle pit and extends to the south for 1000m. The 2-D inversion of chargeability data indicates a moderate chargeability high beginning at a shallow depth starting at the northern end of the line and extending for 200m to the south. The high chargeability anomaly is roughly triangular in shape, with the apex to the south and a depth extent of 200m, giving a distinct impression that sulphide mineralization is pinching out in the southern direction. The resistivity section is similar to the chargeability indicating that the anomalous areas are both chargeable and resistors, which is abnormal for the area.

Line 3000E: This line runs along the northwestern edge of the Ingerbelle pit and the both chargeability and resistivity sections indicate subdued responses indicating that mineralization is unlikely to extend from the pit in a northwest section, except for the southernmost part of the line where a weak chargeability anomaly is present.

Line 4000E: This line runs in a north-northwest direction to the south east of the Ingerbelle pit. A strong bowl-shaped chargeability high occurs in the northern half of the line which

corresponds with a southeast extension of Ingerbelle mineralization. That the chargeability anomaly does not come to surface except where there is bedrock, likely reflects the presence of talus and fill. However, the depth limitation of the chargeability response is somewhat surprizing given the typical vertical extent of mineralization but may be an artefact of processing. Drill data in this area is not deep enough validate the graphical interpretation of the data. A sharp boundary on the southern end of the chargeability high may reflect a fault. Resistivity data is both noisy and subdued and is difficult to directly correlate with chargeability response.

Line 5000E: Is a north-south oriented line cutting across the Similkameen canyon slope approximately halfway between the Copper Mountain super-pit and the Similkameen River. A bowl-shaped, strong, chargeability anomaly that is about 250m wide and 300m deep occurs near the southern end of the line, and is, more or less, on trend with mineralization along the Copper Mountain Stock in the Pit 1 and Pit 3 areas of the Superpit, and the Ingerbelle pit. Relatively abrupt vertical boundaries to the chargeability anomaly is suggestive of fault contacts on the edges of mineralization. The resistivity data is subdued.

Line 6000E: Is also a north-south oriented line that is 200m east of L5000E at the south end but comes to within 50m of the north end of L5000E and continues to the north for 400m. The chargeability response on the south end of the line is similar, but weaker, than the response on L5000E. A shallow, tabular shaped, chargeability high on the north end of the line together with spotty high resistivity responses may be caused by interference from the old conveyor system which runs both proximal and subparallel to L6000E.

Line 7000E: is the easternmost line of the survey area and is oriented on a 010^{o}-190^{o} trend. This line picks up a weak to moderate, "blind" chargeability anomaly on the north end which correlates with the Orinoco anomaly defined by an earlier Titan 24 IP survey. In the central part of the line a relatively small, blind to surface, disk shaped anomaly indicates the western end of Pit 2 mineralization (which was originally thought to be connected to Ingerbelle mineralization and one of the reasons for carrying out the survey). Pit 1 mineralization is likely reflected in the strong chargeability anomaly on the southern end of the survey line. The resistivity section is noisy near surface which may reflect varying depths of fill. A notable vertical divide between response in the north and south, possibly reflects a geological contact Lost Horse Intrusions to the north and Nicola Group rocks to the south. The conductive zone on the northern end of the line is better interpreted from the resistivity plan, and suggests a fault zone – a feature also indicated by extremely difficult drilling conditions in that area.

4.2 Plan Views of Interpreted Chargeability and Resistivity Models

Three dimensional models, of the direct current (DC) resistivity and induced polarization (IP) were carried out utilizing UBC-Geophysical Inversion Facility (UBC-GIF) DCIP3D inversion algorithms. The models can be sliced and diced in any orientation but plan views of various depths below the current topographic surface are used herein and contained in appendix III.

The near surface plans of chargeability display some interesting features a few of which are notable. Four, north-easterly oriented, faults that are approximately evenly spaced between 300-400m apart cut diagonally through the plan view and can be observed to "cut" or bound chargeability anomalies and are reflected in resistivity lows (Fig. 5.1). In general, the chargeability highs correlate to known mineralization, but the location of the chargeability high in the southeast corner of the survey area appears to be offset to the south, and is in an area with no drill control. The chargeability anomalies generally conform to geological understanding and display possible fault boundaries, some of these faults have been mapped in areas of outcrop but were not previously considered continuous nor as significant in controlling mineralization. The linear, south-southeast trending chargeability anomalies in the northeast corner of the map area reflect the historical ore conveyor that used to transport ore from the Copper Mountain pits to the Ingerbelle mill site. Resistivity models are harder to interpret. In some cases, chargeability highs correlate with low resistivity areas and in other cases there are co-incident chargeability and resistivity highs. In the Ingerbelle area, the resistivity high is situated slightly south of the chargeability high with only a small overlap which may reflect the influence of the pit wall on the resistivity response or may reflect underlying geology, either lithology or fracture intensity and moisture content. Comparison of chargeability and resistivity in the southeast part of the survey area which is slightly south and east of the Pit 1 area, is problematic as there is no direct correlation to known geology or mineralization.

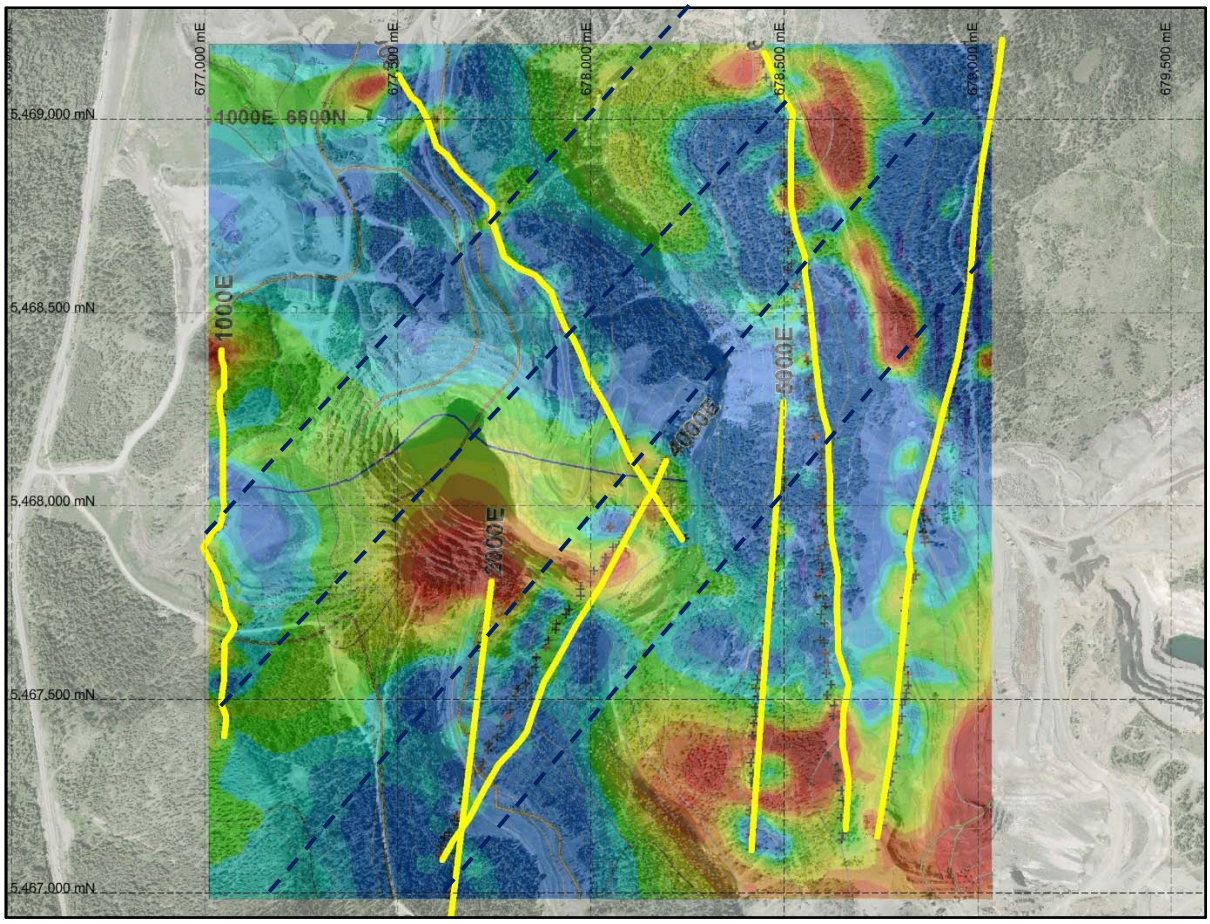

Figure 4.1: Interpreted chargeability Inversion model at 50m below surface topography superimposed on 2007 orthophoto. Yellow lines are survey lines and the blue dashed lines are (interpreted and /or possible) faults.

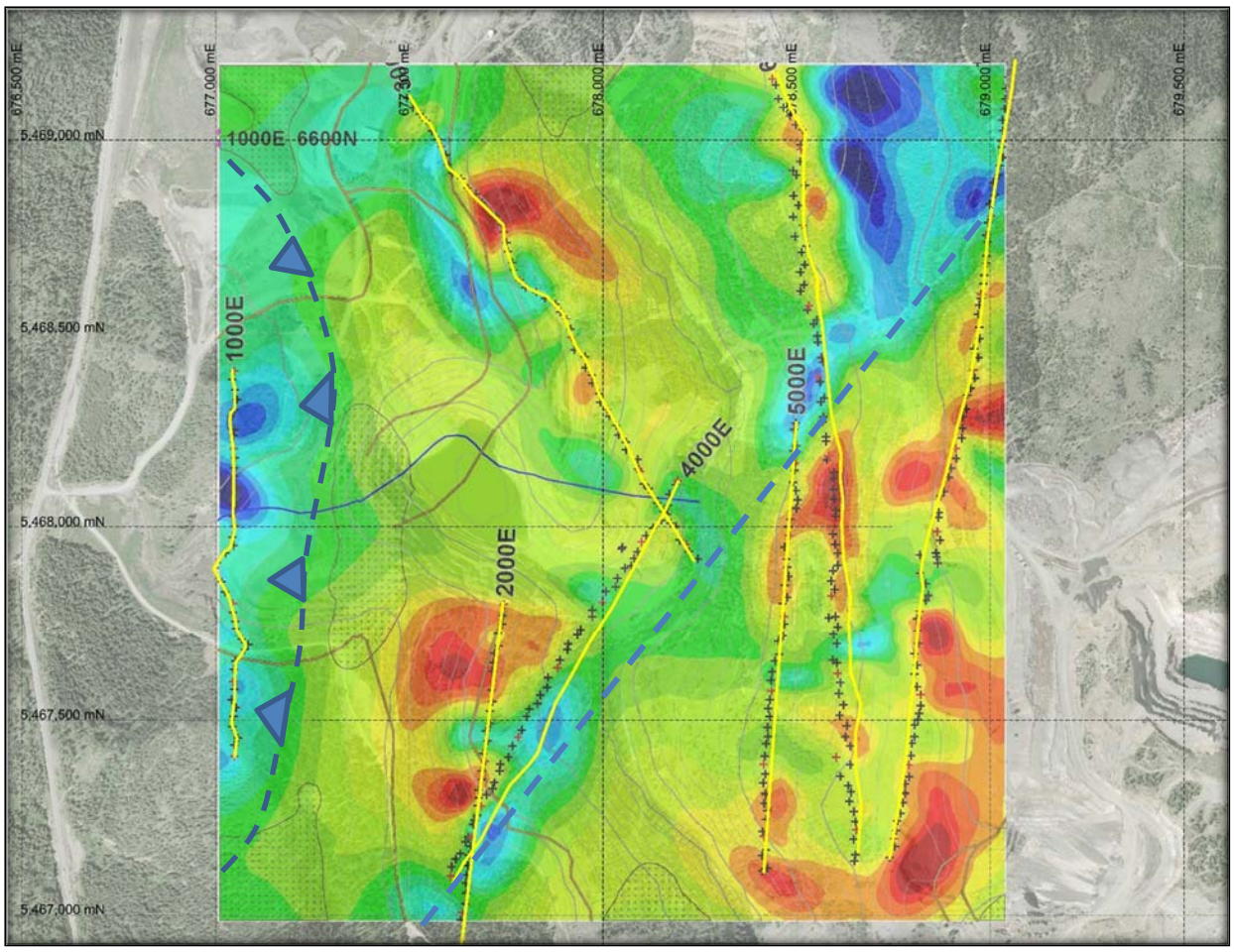

Figure 4.2: Interpreted resistivity inversion model at 75m below surface topography. Yellow lines represent survey lines and the dashed blue line indicates an interpreted fault triangles indicate down-thrust direction.

5. Conclusions

The data from the Volterra 2D-3D IP survey demonstrates that it is a reasonably cost-effective exploration tool in difficult terrain. In general, there is reasonable correlation between chargeability highs and areas of known mineralization with some areas of moderate chargeability that have no drill information and therefore await testing. Magnetic data in the area between Highway 3 and the Ingerbelle deposit suggests that the Boundary Fault is further to the west than placed on most maps and that a thin thrust-slice of sedimentary rocks overlie this area allowing for the possibility of westward continuation of the Ingerbelle mineralization under the thrust slice. However, IP line 1000E displays little indication of disseminated sulphide mineralization at depth. The 3D chargeability image indicates that weak to moderate chargeable rocks may extend to the northwest and southwest of the chargeability high situated along the southern edge of the Ingerbelle pit.

References

BARR. D.A., FOX, P.E., NORTHCOTE, K.E., AND PRETO, V.A.G., 1976. The alkaline suite porphyry deposits – A summary. In Porphyry Deposits of the Canadian Cordillera. Edited by A. Sutherland Brown. Canadian Institute of Mining and Metallurgy, Special Volume 15, pp. 359-367.

DOLMAGE, V. , 1934, Geology and Ore Deposits of Copper Mountain, British Columbia. Geological Survey of Canada Memoir 171.

FAHRNI, K.C., MACAULEY, T.N. AND PRETO, V.A.G., 1976. Copper Mountain and Ingerbelle. In Porphyry Deposits of the Canadian Cordillera. Edited by A. Sutherland Brown. Canadian Institute of Mining and Metallurgy, Special Volume 15, pp. 368-375.

HENDERSON, N., 2010, The Ore Minerals of the Copper Mountain Deposit, Princeton, British Columbia. Unpublished B.Sc. thesis, The University of British Columbia, Okanogan.

GIROUX, G.H., and Holbek, P.M., 2009, Technical Report on the Copper Mountain Project, Princeton, B.C. Copper Mountain Mining Corp. 43:101 Technical Report filed in Sedar.

LANG, J.R.,1993. Petrography and preliminary geochemical evaluation of igneous rocks in the Copper Mountain district. In Annual Technical Report, Year 2, Copper Gold Porphyry Systems of British Columbia, Mineral Deposit Research Unit internal report, The University of British Columbia, Chapter 4.

LOGAN, J. M., and Mihalynuk, M.G., 2013, Tectonic controls on Early Mesozoic paired alkaline porphyry deposit belts (Cu-Au +/- Ag-Pt-Pd-Mo) within the Canadian Cordillera. In prep.

LOWELL, J.D., AND GUILBERT, J.M., 1970. Lateral and Vertical Alteration, Mineralization and Zoning in Porphyry Ore Deposits. Econ Geol. Vol. 65, pp. 373-408.

MIHALYNUK, M.G., Logan, J., Friedman, R.M., and Preto, V.A.G., 2010, Age of Mineralization and 'Mine Dikes' at Copper Mountain Alkaline Copper-Gold-Silver Porphyry Deposit (NTS 092H/07), South-Central British Columbia. British Columbia Geological Survey, Geological Fieldwork 2009, Paper 2010-1 p.163-171.

MONGER, J.W.H., 1989. Geology of the Hope map sheet, British Columbia. Geological Survey of Canada, Map 41-1989, 1:250,000 scale.

MONGER, J.W.H., WHEELER, J.O., TIPPER, H.W., GABRIELSE, H., HARMS, T., STRUICK, L.C., CAMPBELL, R.B., DODDS, C. J., GEHRELS, G.E., AND O'BRIAN, J., 1992. Upper Devonian to Middle Jurassic Assemblages, Part B. Cordilleran Terranes In The

geology of the Cordilleran Orogen in Canada, Edited by H. Gabrielse and C.J. Yorath, Geological Survey of Canada, The Geology of Canada, No. 4, DNAG Vol. G2, pp. 281-328.

MASSEY, N.W.D., VINEHAM, J.M.S., OLIVER, S.L., 2009. Southern Nicola Project: Whipsaw Creek-Eastgate-Wolfe Creek Area, Southern British Columbia (NTS 092H/01W, 02E, 07E, 08W). Geological Fieldwork 2008, Paper 2009-1 BC Ministry of Energy, Mines and Petroleum Resources.

MONTGOMERY, J.H., 1968. Petrology, Structure and Origin of the Copper Mountain Intrusions near Princeton, B.C. Unpublished PhD Thesis, The University of British Columbia, 175 p.

PRETO, V.A.G., 1972. Geology of Copper Mountain. British Columbia Department of Energy Mines and Petroleum Resources, Bulletin 59, 87 pages.

PRETO, V.A.G., 1977. The Nicola Group: Mesozoic Volcanism Related to Rifting in Southern British Columbia. In Volcanic Regimes in Canada, edited by Baragar, W.R.A., Coleman, L.C. and Hall, J.M., Geological Association of Canada Special Paper No. 16 pp. 39-57

PRETO, V.A.G., 1979. Geology of the Nicola Group between Merritt and Princeton. B.C.E.M.P.R. Bull. No. 69.

SJ GEOPHYSICS, 2017. Logistics Report prepared for Copper Mountain Mining Corp. on the 2D and 3D Induced Polarization Survey, Similkameen Canyon. Unpublished Company Report.

STANLEY, C.R., HOLBEK, P. M., HUYCK, H.L., LANG, J.R., PRETO, V.A.G., BLOWER, S.J., AND BOTTARO, J.C., 1996. Geology of the Copper Mountain alkalic copper-gold porphyry deposits, Princeton, British Columbia. In Porphyry Deposits of the Northwestern Cordillera of North America. Canadian Institute of Mining and Metallurgy, Special Volume 46, pp. 537-565.

WOODSWORTH, G.J., ANDERSON, R.G., ARMSTRONG, R.L., STRUICK, L.C., AND VAN DER HEYDEN, P., 1992. Plutonic regimes. In The Geology of the Cordilleran Orogen in Canada. Edited by H. Gabrielse and C.J. Yorath, Geological Survey of Canada, The Geology of Canada, No. 4, DNAG Vol. G2, pp. 493-531.

Statement of Expenditures

Geophysical Survey (May 29th to June 9th incl. travel)	$60,351.74
Geophysical Data Processing and documentation	$10,914.75
Project Planning, Supervision and Logistics	$ 2,640.00
Subtotal	$75,706.49
	==========
Apply 39% of Geophysical survey area on mineral claims	$ 29,525.31
26% of Lidar Survey (at $22,050.00)	$ 5,733.00
Lidar data processing	$ 1,800.00
Report	$ 2,600.00
	==========
Total	$ 39,658.31

Statement of Qualifications

I, Peter M. Holbek with a business address of 1700 – 700 West Pender Street, Vancouver, British Columbia, V6C 1G8, do hereby certify that:

1. I am a professional geologist registered under the Professional Engineers and Geoscientists Act of the Province of British Columbia and a member in good standing with the Association of Professional Engineers and Geoscientists of British Columbia.
2. I am a graduate of The University of British Columbia with a B.Sc. in geology 1980 and an M.Sc. in geology, 1988.
3. I have practiced my profession continuously since 1980.
4. I am Vice President, Exploration for Copper Mountain Mining Corp. having a business address as given above.
5. I was on-site during the geophysical survey period at the Copper Mountain Mine.

__"signed"_____
Peter Holbek, M.Sc., P.Geo.

Appendix 1: Claim Listing

TABLE 3: Mineral Claim Current Status - Copper Mountain Property, BC
Copper Mountain Mine (BC) Ltd.
Client No. – 141588

Title Number	Claim Name	Map Number	Issue Date	Good To Date	Status	Area (ha)
248598	ROAD	092H038	1976/APR/08	2024/NOV/30	GOOD	75.0
248603	SIMCOL #1 FR.	092H038	1976/NOV/05	2026/NOV/30	GOOD	25.0
248604	SIMCOL #2 FR.	092H038	1976/NOV/05	2026/NOV/30	GOOD	25.0
248605	SIMCOL #10	092H038	1976/NOV/05	2024/NOV/30	GOOD	100.0
248606	SIMCOL #11	092H038	1976/NOV/05	2024/NOV/30	GOOD	25.0
248609	NEWMIN #1	092H038	1977/MAR/24	2022/NOV/30	GOOD	500.0
248610	NEWMIN #2	092H038	1977/MAR/24	2022/NOV/30	GOOD	400.0
248626	NEWMIN #3	092H038	1978/FEB/02	2022/NOV/30	GOOD	225.0
248627	NEWMIN #4	092H038	1978/FEB/02	2022/NOV/30	GOOD	50.0
248628	NEWMIN #5	092H038	1978/FEB/02	2022/NOV/30	GOOD	75.0
248640	DOT FR	092H038	1978/JUN/20	2023/APR/26	GOOD	25.0
248723	ALPINE #1	092H038	1979/JUL/20	2023/APR/26	GOOD	75.0
248724	ALPINE FR.	092H038	1979/JUL/20	2023/APR/26	GOOD	25.0
248778	BULLET #1 FR.	092H038	1979/NOV/27	2023/APR/26	GOOD	25.0
248779	BULLET #2 FR.	092H038	1979/NOV/27	2022/APR/26	GOOD	25.0
248782	REFER TO LOT TABLE	092H038	1979/DEC/21	2022/OCT/26	GOOD	25.0
248783	NM #1 FR.	092H038	1979/DEC/28	2024/OCT/26	GOOD	25.0
248784	NM #2 FR.	092H038	1979/DEC/28	2022/APR/26	GOOD	25.0
248785	NM #3 FR.	092H038	1979/DEC/28	2022/APR/26	GOOD	25.0
248786	NM #4 FRACTION	092H038	1979/DEC/28	2022/APR/26	GOOD	25.0
248787	NM #5 FR.	092H038	1979/DEC/28	2022/APR/26	GOOD	25.0
248788	NM #6 FR.	092H038	1979/DEC/28	2022/OCT/26	GOOD	25.0
248809	LAN NO.1	092H038	1980/MAY/28	2022/NOV/30	GOOD	50.0
248810	LAN NO.2	092H038	1980/MAY/28	2022/NOV/30	GOOD	25.0
248811	LAN NO.3	092H038	1980/MAY/28	2022/NOV/30	GOOD	150.0
248812	LAN NO.4	092H038	1980/MAY/28	2022/NOV/30	GOOD	100.0
248813	LAN NO.5	092H038	1980/MAY/28	2022/NOV/30	GOOD	50.0
248814	LAN NO.6	092H038	1980/MAY/28	2022/NOV/30	GOOD	50.0
248815	LAN NO.7	092H038	1980/MAY/28	2022/NOV/30	GOOD	50.0
249233	ALPINE 3	092H038	1987/JUL/24	2020/APR/26	GOOD	500.0
249234	ALPINE 4	092H038	1987/JUL/24	2020/APR/26	GOOD	500.0
249235	ALPINE 5	092H038	1987/JUL/24	2022/APR/26	GOOD	25.0
249264	ALPINE 6 FR	092H038	1987/OCT/08	2022/APR/26	GOOD	25.0
249265	ALPINE 7 FR	092H038	1987/OCT/08	2022/APR/26	GOOD	25.0
250157	PENNY NO. 1 FR.	092H038	1955/APR/01	2023/APR/26	GOOD	25.0
250159	MAY #1	092H038	1961/MAR/21	2022/APR/26	GOOD	25.0
250161	MAY #5 FR.	092H038	1961/SEP/01	2022/APR/26	GOOD	25.0
250164	RAY NO. 7	092H038	1962/JUN/27	2022/APR/26	GOOD	25.0
250165	RAY NO. 8	092H038	1962/JUN/27	2022/APR/26	GOOD	25.0
250166	QUEEN D. FR.	092H038	1963/JUL/08	2022/APR/26	GOOD	25.0
250167	QUEEN E. FR.	092H038	1963/JUL/08	2022/APR/26	GOOD	25.0
250168	QUEEN G. FR.	092H038	1963/JUL/08	2022/APR/26	GOOD	25.0

250169	QUEEN H. FR.	092H038	1963/JUL/08	2022/APR/26	GOOD	25.0
250170	QUEEN J. FR.	092H038	1963/JUL/08	2022/APR/26	GOOD	25.0
250171	QUEEN B. FR.	092H038	1963/JUL/05	2022/APR/26	GOOD	25.0
250172	QUEEN A. FR.	092H038	1963/JUL/05	2022/APR/26	GOOD	25.0
250173	QUEEN C. FR.	092H038	1963/JUL/05	2022/APR/26	GOOD	25.0
250174	R.R. FR.	092H038	1963/JUL/22	2022/NOV/30	GOOD	25.0
250175	R FR.	092H038	1963/AUG/22	2022/NOV/30	GOOD	25.0
250176	ELEPHANT NO.1	092H038	1963/SEP/11	2023/APR/26	GOOD	25.0
250177	ELEPHANT NO. 2 FR.	092H038	1963/SEP/11	2022/APR/26	GOOD	25.0
250178	ELEPHANT NO. 3	092H038	1963/SEP/11	2022/APR/26	GOOD	25.0
250179	ELEPHANT NO. 4	092H038	1963/SEP/11	2023/APR/26	GOOD	25.0
250182	"E.M." FR	092H038	1964/DEC/14	2023/APR/26	GOOD	25.0
250185	"BEM" NO.1	092H038	1964/DEC/23	2023/APR/26	GOOD	25.0
250186	"BEM" NO.3	092H038	1964/DEC/23	2022/APR/26	GOOD	25.0
250187	"BEM" NO.5	092H038	1964/DEC/23	2022/APR/26	GOOD	25.0
250188	"BEM" NO.7	092H038	1964/DEC/23	2023/APR/26	GOOD	25.0
250195	RAD NO.1	092H038	1965/MAY/26	2022/JAN/15	GOOD	25.0
250196	RAD NO.2	092H038	1965/MAY/26	2022/JAN/15	GOOD	25.0
250197	RAD NO.3	092H038	1965/MAY/26	2022/APR/26	GOOD	25.0
250198	RAD NO.4	092H038	1965/MAY/26	2022/APR/26	GOOD	25.0
250199	RAD NO.5	092H038	1965/MAY/26	2022/APR/26	GOOD	25.0
250200	RAD NO.6	092H038	1965/MAY/26	2022/APR/26	GOOD	25.0
250201	RAD NO.7	092H038	1965/MAY/26	2022/APR/26	GOOD	25.0
250202	RAD NO.8	092H038	1965/MAY/26	2022/APR/26	GOOD	25.0
250204	RAD NO.10	092H038	1965/MAY/26	2022/APR/26	GOOD	25.0
250205	BRIAN H. FR.	092H038	1965/JUL/26	2022/APR/26	GOOD	25.0
250206	SER #3	092H038	1965/NOV/30	2022/APR/26	GOOD	25.0
250207	SER #4	092H038	1965/NOV/30	2022/APR/26	GOOD	25.0
250208	SER #5	092H038	1965/NOV/30	2022/APR/26	GOOD	25.0
250209	SER #6	092H038	1965/NOV/30	2022/APR/26	GOOD	25.0
250210	SER #7	092H038	1965/NOV/30	2022/APR/26	GOOD	25.0
250211	SER #8	092H038	1965/NOV/30	2022/APR/26	GOOD	25.0
250212	SER #9	092H038	1965/NOV/30	2022/APR/26	GOOD	25.0
250213	SER #10	092H038	1965/NOV/30	2022/APR/26	GOOD	25.0
250214	SER #11	092H038	1965/NOV/30	2022/APR/26	GOOD	25.0
250215	SER #12	092H038	1965/NOV/30	2022/APR/26	GOOD	25.0
250216	SER #13	092H038	1965/NOV/30	2020/APR/26	GOOD	25.0
250217	SER #14	092H038	1965/NOV/30	2022/APR/26	GOOD	25.0
250218	SER #15	092H038	1965/NOV/30	2022/APR/26	GOOD	25.0
250219	SER #16	092H038	1965/NOV/30	2022/APR/26	GOOD	25.0
250220	SER #17	092H038	1965/NOV/30	2022/APR/26	GOOD	25.0
250221	SER #18	092H038	1965/NOV/30	2022/APR/26	GOOD	25.0
250222	SER #19 FR.	092H038	1965/NOV/30	2022/APR/26	GOOD	25.0
250223	SER #20	092H038	1965/NOV/30	2022/APR/26	GOOD	25.0
250224	SER #21 FR.	092H038	1965/NOV/30	2022/APR/26	GOOD	25.0
250225	SER #22	092H038	1965/NOV/30	2022/APR/26	GOOD	25.0
250226	SER #23	092H038	1965/NOV/30	2022/APR/26	GOOD	25.0
250227	SER #24 FR.	092H038	1965/NOV/30	2022/APR/26	GOOD	25.0
250228	SER #25 FR.	092H038	1965/NOV/30	2022/APR/26	GOOD	25.0

250229	NUT #7	092H038	1966/FEB/18	2022/APR/26	GOOD	25.0
250230	NUT #8	092H038	1966/FEB/18	2022/APR/26	GOOD	25.0
250231	NUT #9	092H038	1966/FEB/18	2022/APR/26	GOOD	25.0
250232	NUT #10	092H038	1966/FEB/18	2022/APR/26	GOOD	25.0
250233	NUT #11	092H038	1966/FEB/18	2022/APR/26	GOOD	25.0
250235	NUT #13	092H038	1966/FEB/18	2020/APR/26	GOOD	25.0
250236	NUT #14	092H038	1966/FEB/18	2022/APR/26	GOOD	25.0
250240	RAY 13 FR	092H038	1965/MAY/27	2022/APR/26	GOOD	25.0
250243	COPPER BLUFF FR.	092H038	1966/AUG/15	2022/APR/26	GOOD	25.0
250244	MCB #1	092H038	1966/SEP/13	2022/APR/26	GOOD	25.0
250245	MCB #2	092H038	1966/SEP/13	2022/APR/26	GOOD	25.0
250246	MCB #3	092H038	1966/SEP/13	2022/APR/26	GOOD	25.0
250247	MCB #4	092H038	1966/SEP/13	2022/APR/26	GOOD	25.0
250248	MCB #5	092H038	1966/SEP/13	2022/APR/26	GOOD	25.0
250249	MCB #6	092H038	1966/SEP/13	2022/APR/26	GOOD	25.0
250250	DEEP #1	092H038	1967/MAR/16	2022/APR/26	GOOD	25.0
250251	DEEP #2	092H038	1967/MAR/16	2022/APR/26	GOOD	25.0
250252	DEEP #3	092H038	1967/MAR/16	2022/APR/26	GOOD	25.0
250253	DEEP #4	092H038	1967/MAR/16	2022/APR/26	GOOD	25.0
250254	DEEP #5	092H038	1967/MAR/16	2022/APR/26	GOOD	25.0
250255	DEEP #6	092H038	1967/MAR/16	2022/APR/26	GOOD	25.0
250256	DEEP #7	092H038	1967/MAR/16	2022/APR/26	GOOD	25.0
250257	DEEP #8	092H038	1967/MAR/16	2022/APR/26	GOOD	25.0
250258	DEEP #9	092H038	1967/MAR/16	2022/APR/26	GOOD	25.0
250259	DEEP #10	092H038	1967/MAR/16	2022/APR/26	GOOD	25.0
250260	AF 13	092H038	1967/MAR/31	2022/NOV/30	GOOD	25.0
250261	AF 14	092H038	1967/MAR/31	2022/NOV/30	GOOD	25.0
250262	FRIEDA FR	092H038	1967/JUN/08	2022/APR/26	GOOD	25.0
250268	ANNIE FR.	092H038	1967/AUG/01	2022/APR/26	GOOD	25.0
250269	RAD #1 FR.	092H038	1967/NOV/24	2022/APR/26	GOOD	25.0
250270	BETH #1 FR	092H038	1967/DEC/01	2022/APR/26	GOOD	25.0
250271	BETH #2 FR	092H038	1967/DEC/01	2022/APR/26	GOOD	25.0
250272	BETH #3 FR	092H038	1967/DEC/01	2022/APR/26	GOOD	25.0
250273	BETH #5 FR	092H038	1967/DEC/01	2022/JAN/15	GOOD	25.0
250274	BETH #4 FR	092H038	1967/DEC/22	2022/JAN/15	GOOD	25.0
250275	BETH #6 FR	092H038	1967/DEC/22	2022/APR/26	GOOD	25.0
250276	BETH #7 FR	092H038	1967/DEC/22	2022/APR/26	GOOD	25.0
250277	BETH #8 FR.	092H038	1968/FEB/05	2022/JAN/15	GOOD	25.0
250278	BETH #9 FR.	092H038	1968/FEB/23	2022/APR/26	GOOD	25.0
250279	BETH #10 FRACTIONAL	092H038	1968/FEB/27	2022/JAN/15	GOOD	25.0
250280	DEN #1 FR.	092H038	1968/JUL/25	2022/APR/26	GOOD	25.0
250281	DEN #2 FR.	092H038	1968/JUL/25	2022/APR/26	GOOD	25.0
250321	DEEP NO.1 FR	092H038	1971/MAR/23	2022/APR/26	GOOD	25.0
250322	DEEP NO.2 FR	092H038	1971/MAR/23	2022/APR/26	GOOD	25.0
250323	DEEP NO.3 FR	092H038	1971/MAR/23	2022/APR/26	GOOD	25.0
250324	DEEP NO.4 FR	092H038	1971/MAR/23	2022/APR/26	GOOD	25.0
250325	DEEP NO.5 FR	092H038	1971/MAR/23	2022/APR/26	GOOD	25.0
250330	REFER TO LOT TABLE	092H038	1974/NOV/26	2022/NOV/30	GOOD	25.0
301376	WR 1	092H038	1991/JUN/28	2022/APR/26	GOOD	25.0

301377	WR 2	092H038	1991/JUN/28	2022/APR/26	GOOD	25.0
301378	WR 3	092H038	1991/JUN/28	2022/APR/26	GOOD	25.0
301379	WR 4	092H038	1991/JUN/28	2022/APR/26	GOOD	25.0
301380	WR 5	092H038	1991/JUN/28	2022/APR/26	GOOD	25.0
301381	WR 6	092H038	1991/JUN/28	2022/APR/26	GOOD	25.0
301394	WES 1	092H038	1991/JUN/29	2019/APR/26	GOOD	375.0
301395	WES 2	092H028	1991/JUN/29	2019/APR/26	GOOD	375.0
301396	WES 3	092H028	1991/JUN/30	2019/APR/26	GOOD	300.0

Appendix II: Instrument Specifications Volterra Dabtube 24-bit four-channel acquisition unit

Input impedance:	20MΩ
Input overvoltage protection:	5.6V
Internal memory:	Variable USB flash memory stick (currently 64 GB)
Number of inputs:	4 galvanically isolated inputs
Synchronization: Selectable Sampling Rates (samples/second):	GPS 128000, 64000, 32000, 16000, 8000, 4000, 2000, 1000
Common mode rejection:	More than 80dB (for Rs=0)
Voltage sensitivity:	Range: 10V (peak to peak, ± 5V)
Communication:	Resolution: 0.24 μV Bluetooth and USB
Serial Port:	4 RS-232 full duplex
Digital I/O:	6 time stamped ports
Features: **General:**	Programmable Gain, AC/DC Coupling
Dimensions:	Diameter: 43mm, Length: 405mm
Weight: Battery:	0.5kg 5.0VDC nominal
Operating temperature range:	-40°C to 40°C

GDD TxII IP Transmitter

Input Voltage:	120V / 60 Hz or 240V/50 Hz (optional)
Output Power:	3.6 kW maximum
Output Voltage:	150 to 2200V
Output Current:	5 mA to 10A
Time Domain:	1, 2, 4, 8 second on/off cycle
Operating Temp. Range:	-40ºC to +65ºC
Display:	Digital LCD read to 0.001 A
Dimensions:	34 x 21 x 39 cm
Weight:	20Kg

Appendix III: Volterra Geophysical Survey, Data Presentation

GEOPHYSICS
Science on Target

11966 – 95A Avenue,
Delta, BC V4C 3W2 Canada
Tel +1 (604) 582-1100
www.sjgeophysics.com

MEMORANDUM

Date: June 8, 2017

From: Shawn Rastad

To: Richard Joyes, Peter Holbek

SUBJECT: Preliminary 2D inversions – Similkameen Canyon Project

Please find attached a series of pseudosections for the first six lines that were acquired followed by the 2D inverted results. These are to be considered as preliminary as they are the first pass inversion results. These inversions are based on an initial QC and utilize field GPS elevation data. A second QA process is required in an attempt to remove responses associated with culture that may negatively influence the model results.

In addition to the 2D data acquired, the crew did acquire offset currents for each line acquired on the east side of the river. This will allow for a 3D inversion to be completed.

I will be out of the office the remaining of the week and back on Monday. If you have any questions I will be happy to discuss the project and results with you next week.

PSEUDOSECTIONS

otential : P-Line 1000.0E, C-Line 1000.0E : C-Stn < P-Stn : Pole-Dipole : 230 data
Observed Apparent Resistivity

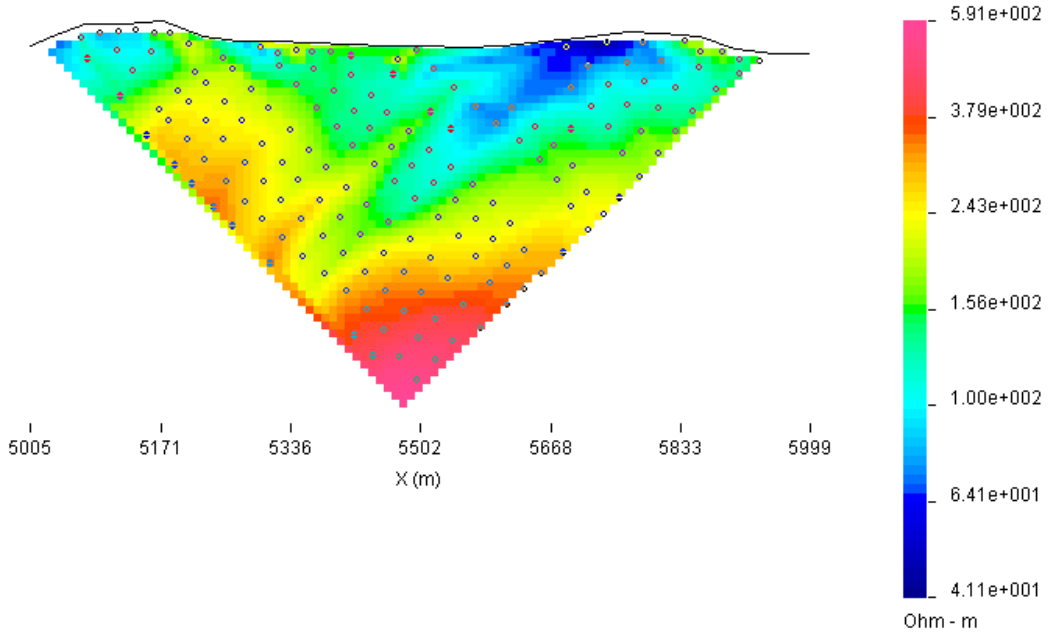

otential : P-Line 1000.0E, C-Line 1000.0E : C-Stn > P-Stn : Pole-Dipole : 232 data
Observed Apparent Resistivity

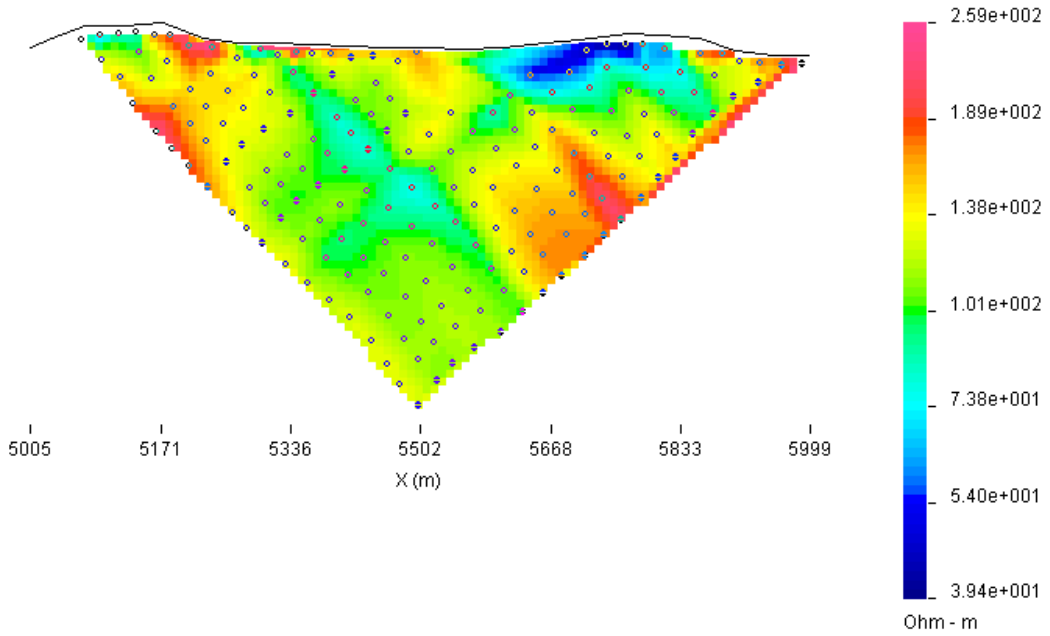

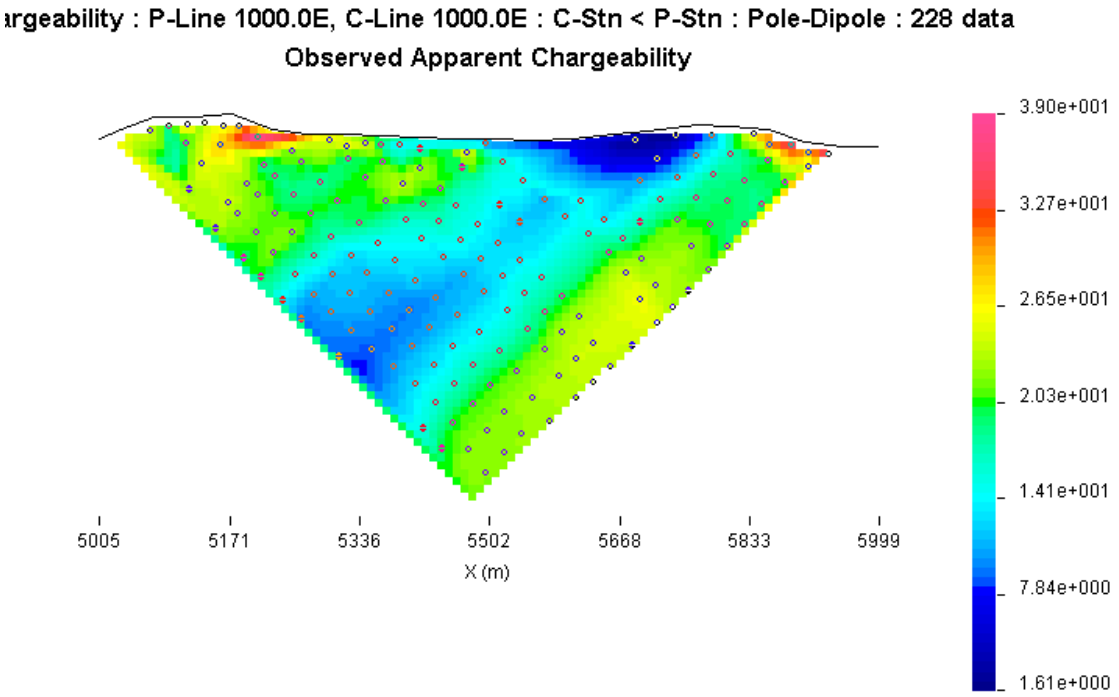
rgeability : P-Line 1000.0E, C-Line 1000.0E : C-Stn < P-Stn : Pole-Dipole : 228 data
Observed Apparent Chargeability
3.90e+001
3.27e+001
2.65e+001
2.03e+001
1.41e+001
7.84e+000
1.61e+000
5005
5171
5336
5502
5668
5833
5999
X (m)

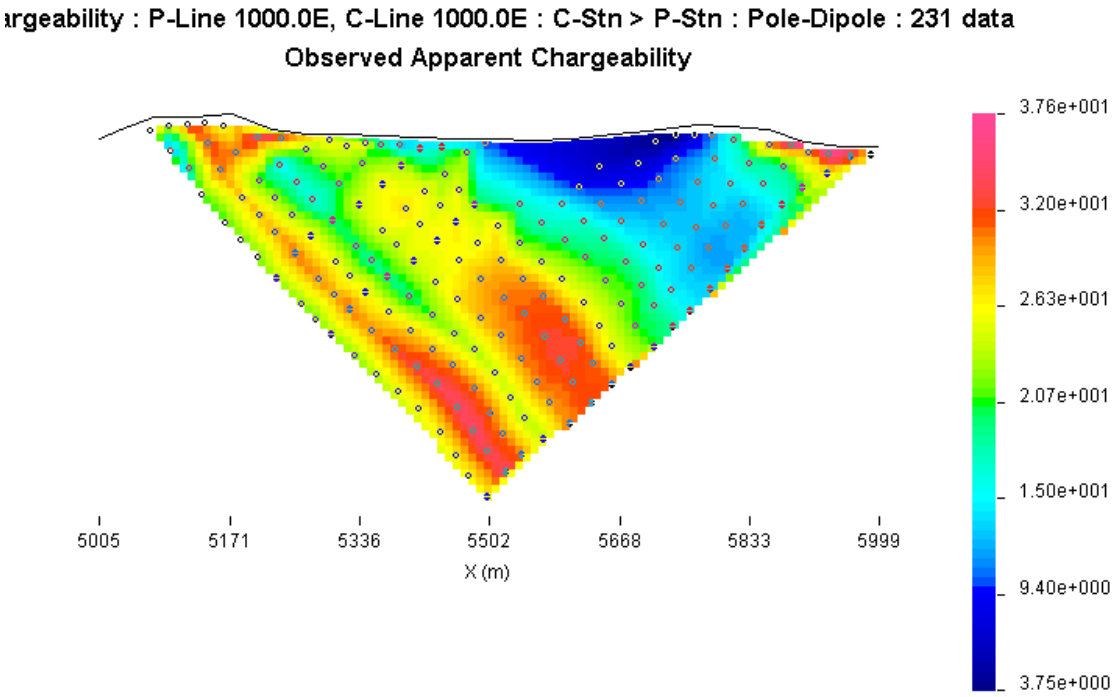
rgeability : P-Line 1000.0E, C-Line 1000.0E : C-Stn > P-Stn : Pole-Dipole : 231 data
Observed Apparent Chargeability
3.76e+001
3.20e+001
2.63e+001
2.07e+001
1.50e+001
9.40e+000
3.75e+000
5005
5171
5336
5502
5668
5833
5999
X (m)

otential : P-Line 2000.0E, C-Line 2000.0E : C-Stn < P-Stn : Pole-Dipole : 294 data

Observed Apparent Resistivity

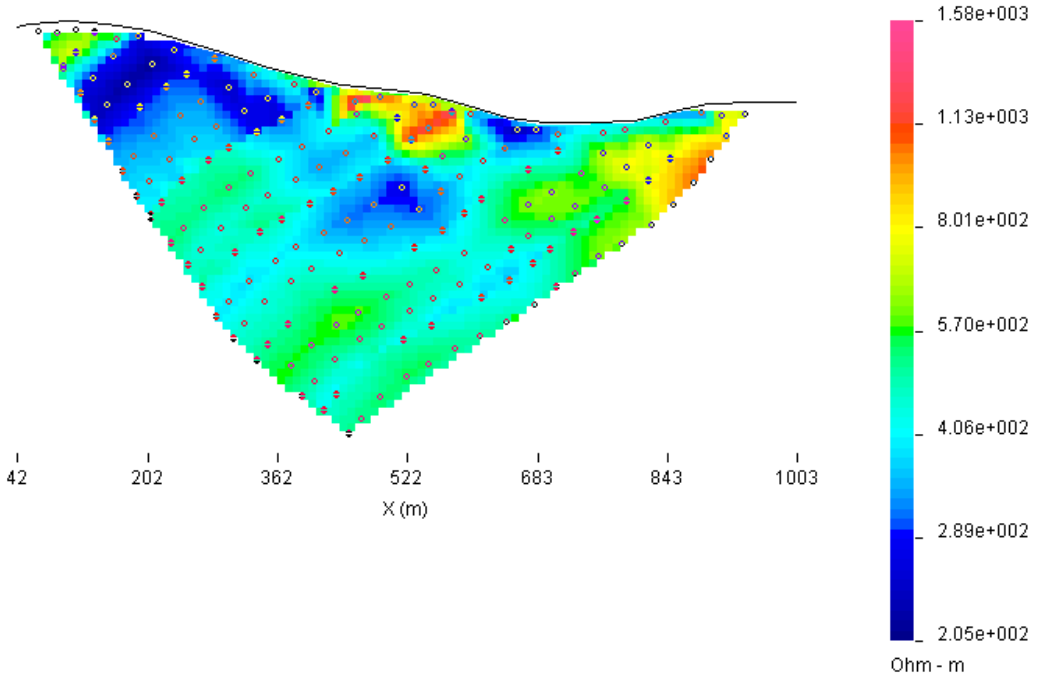

otential : P-Line 2000.0E, C-Line 2000.0E : C-Stn > P-Stn : Pole-Dipole : 271 data

Observed Apparent Resistivity

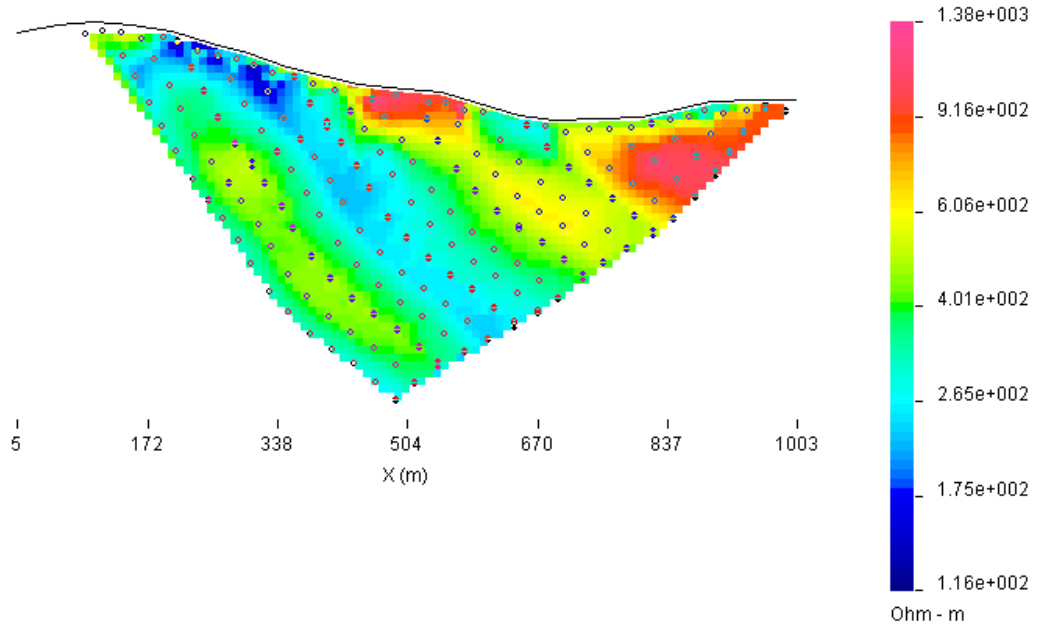

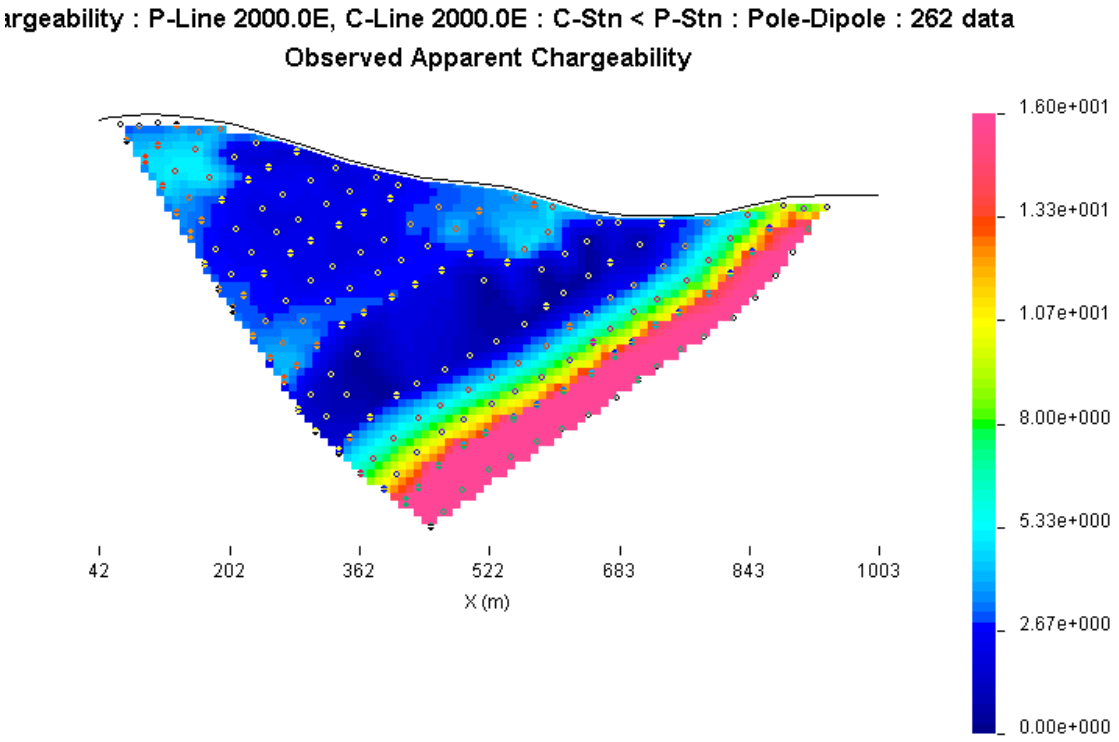
rgeability : P-Line 2000.0E, C-Line 2000.0E : C-Stn < P-Stn : Pole-Dipole : 262 data
Observed Apparent Chargeability
1.60e+001
1.33e+001
1.07e+001
8.00e+000
5.33e+000
2.67e+000
0.00e+000
42
202
362
522
683
843
1003
X (m)

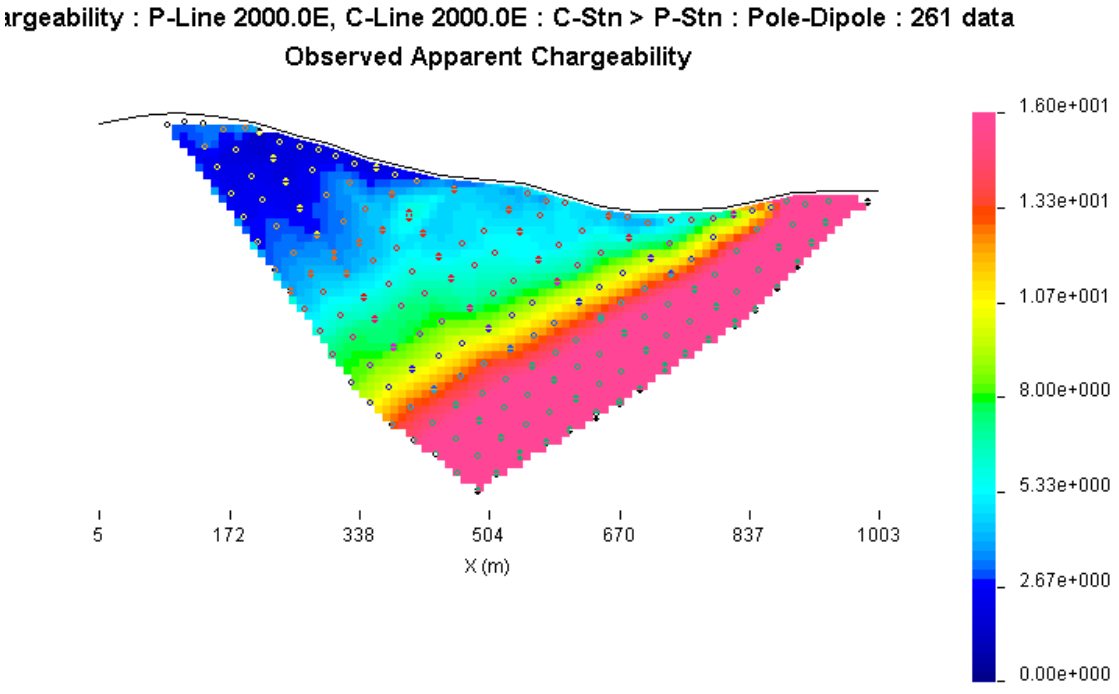
rgeability : P-Line 2000.0E, C-Line 2000.0E : C-Stn > P-Stn : Pole-Dipole : 261 data
Observed Apparent Chargeability
1.60e+001
1.33e+001
1.07e+001
8.00e+000
5.33e+000
2.67e+000
0.00e+000
5
172
338
504
670
837
1003
X (m)

otential : P-Line 3000.0E, C-Line 3000.0E : C-Stn < P-Stn : Pole-Dipole : 658 data
Observed Apparent Resistivity

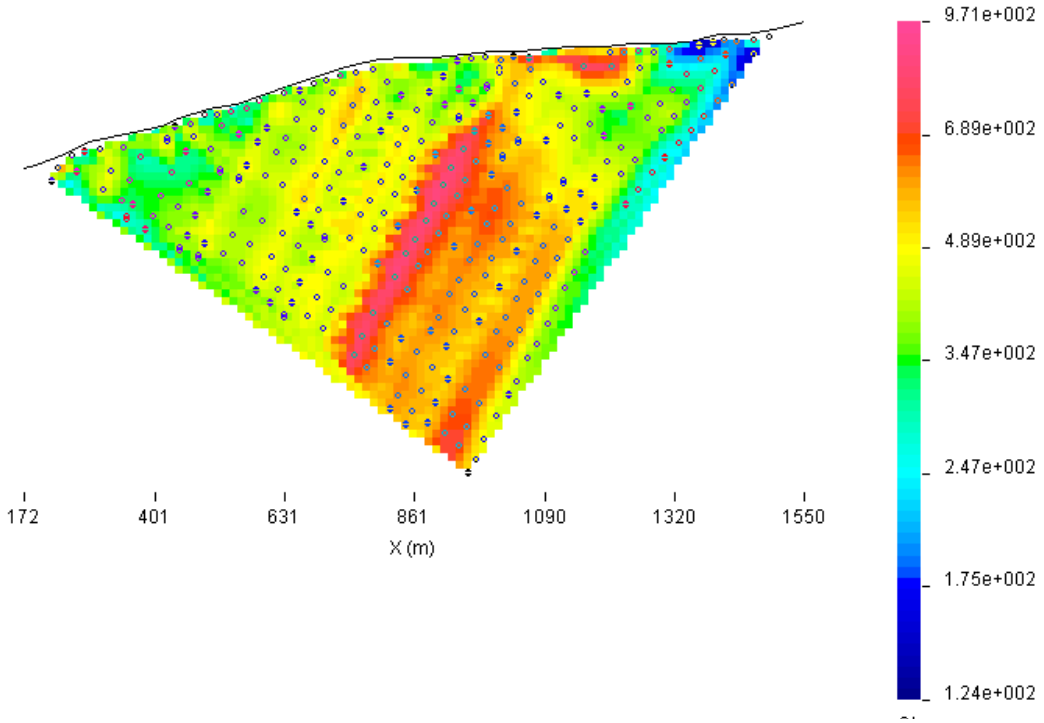

otential : P-Line 3000.0E, C-Line 3000.0E : C-Stn > P-Stn : Pole-Dipole : 661 data
Observed Apparent Resistivity

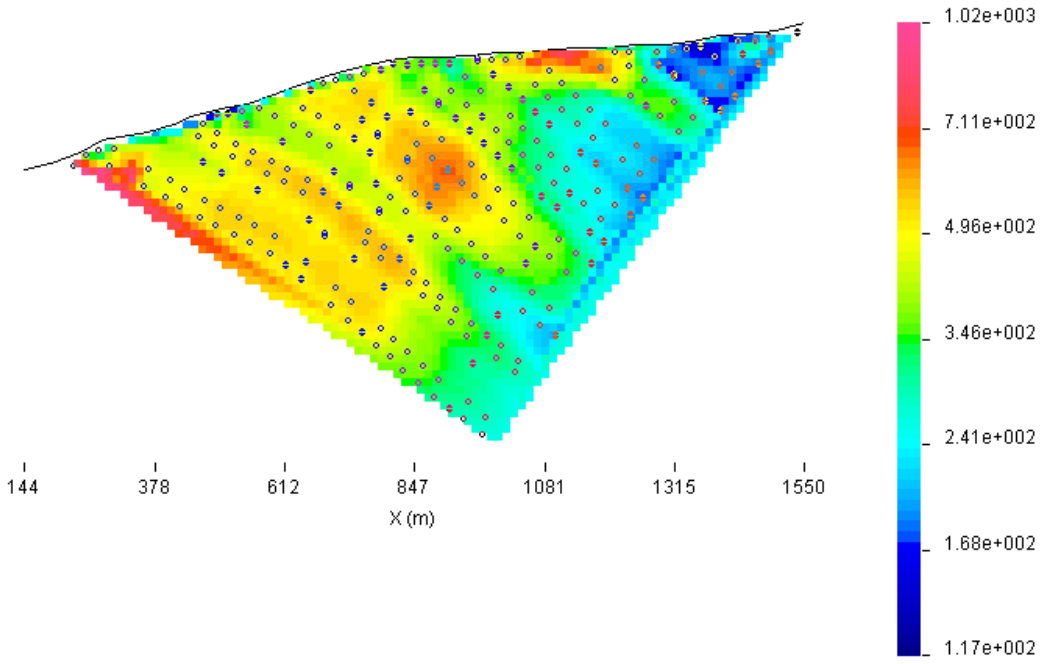

otential : P-Line 5000.0E, C-Line 5000.0E : C-Stn < P-Stn : Pole-Dipole : 336 data

Observed Apparent Resistivity

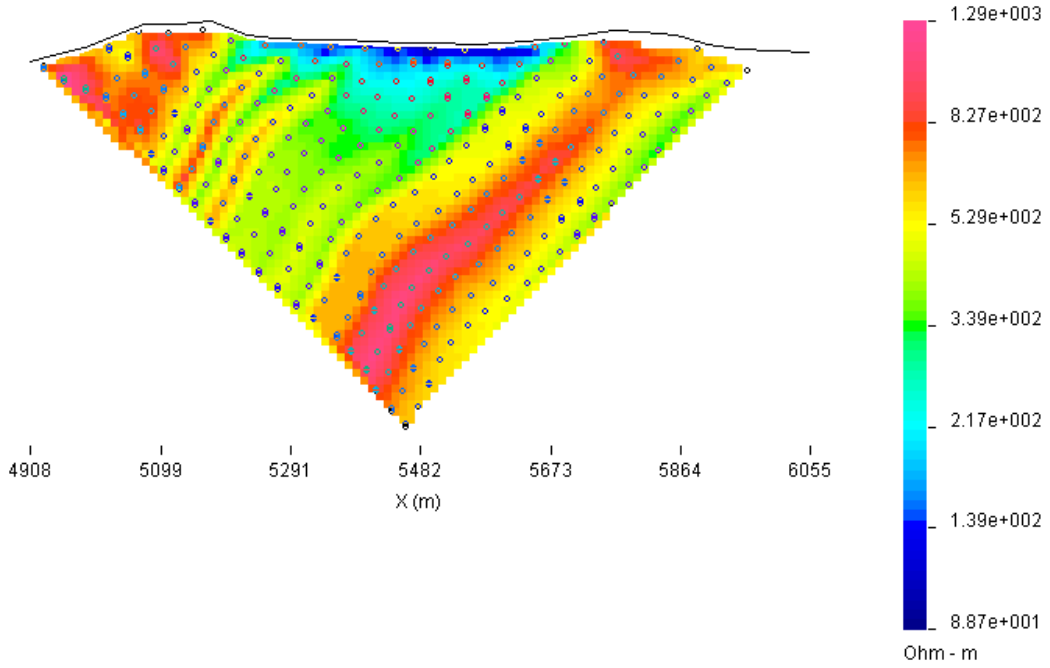

otential : P-Line 5000.0E, C-Line 5000.0E : C-Stn > P-Stn : Pole-Dipole : 319 data

Observed Apparent Resistivity

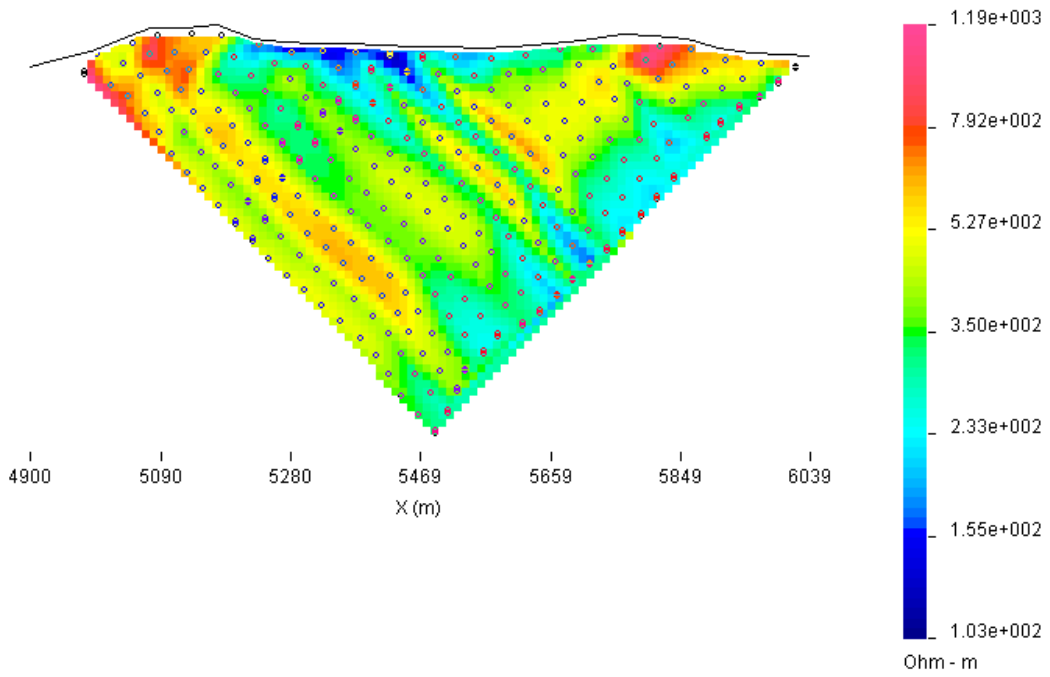

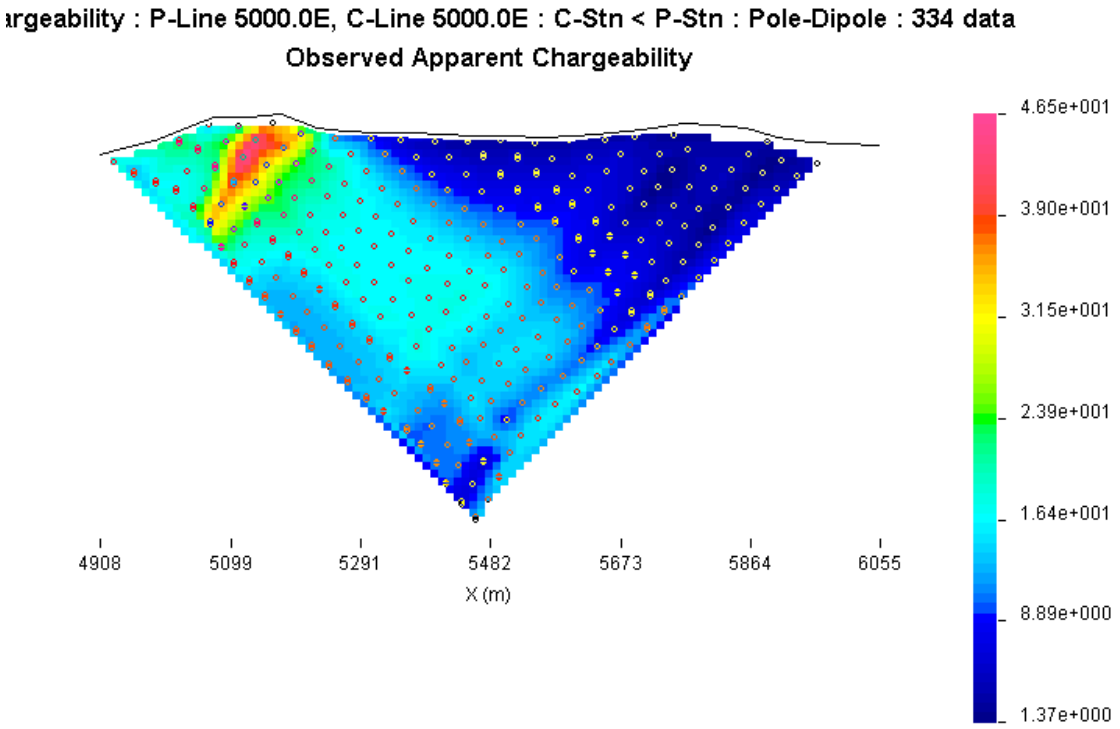
rgeability : P-Line 5000.0E, C-Line 5000.0E : C-Stn < P-Stn : Pole-Dipole : 334 data
Observed Apparent Chargeability
4.65e+001
3.90e+001
3.15e+001
2.39e+001
1.64e+001
8.89e+000
1.37e+000
4908
5099
5291
5482
5673
5864
6055
X (m)

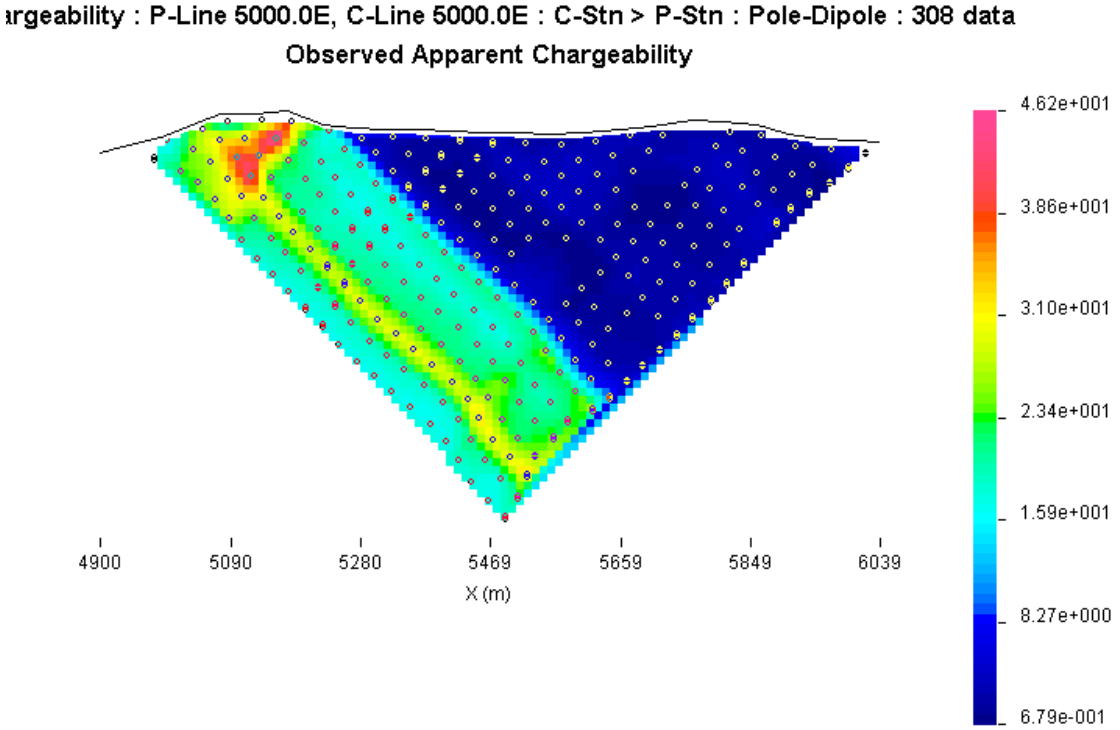
rgeability : P-Line 5000.0E, C-Line 5000.0E : C-Stn > P-Stn : Pole-Dipole : 308 data
Observed Apparent Chargeability
4.62e+001
3.86e+001
3.10e+001
2.34e+001
1.59e+001
8.27e+000
6.79e-001
4900
5090
5280
5469
5659
5849
6039
X (m)

otential : P-Line 6000.0E, C-Line 6000.0E : C-Stn < P-Stn : Pole-Dipole : 908 data

Observed Apparent Resistivity

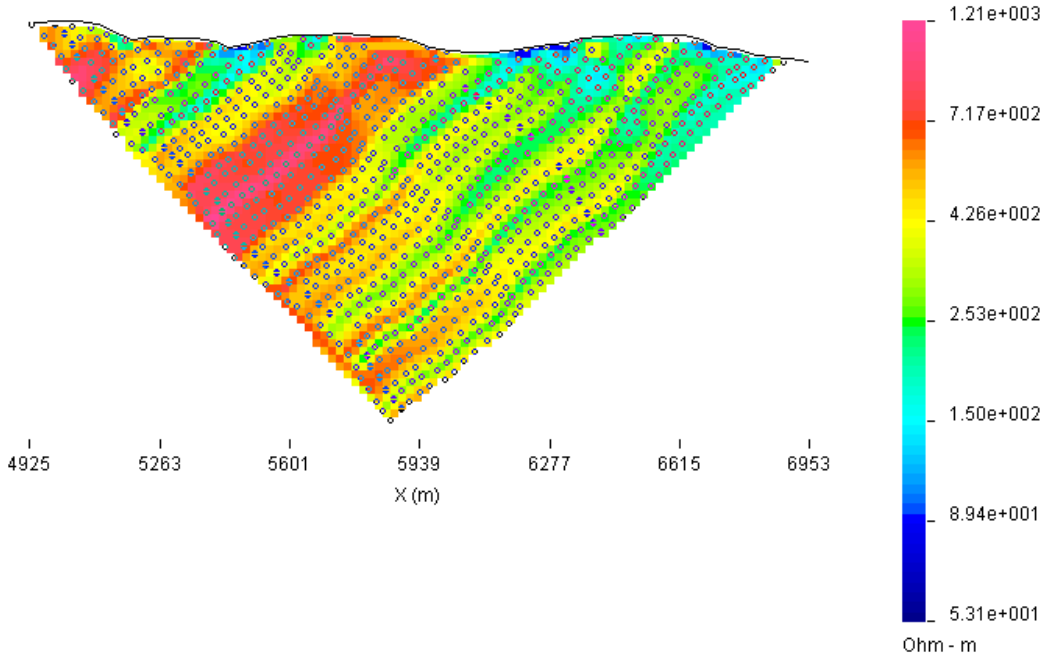

otential : P-Line 6000.0E, C-Line 6000.0E : C-Stn > P-Stn : Pole-Dipole : 823 data

Observed Apparent Resistivity

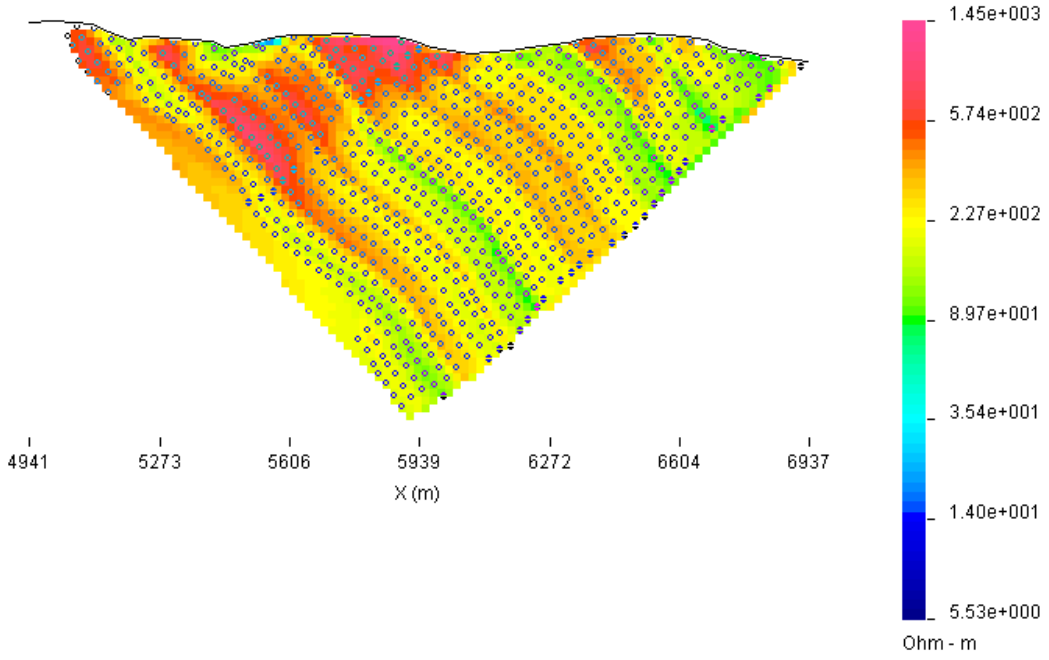

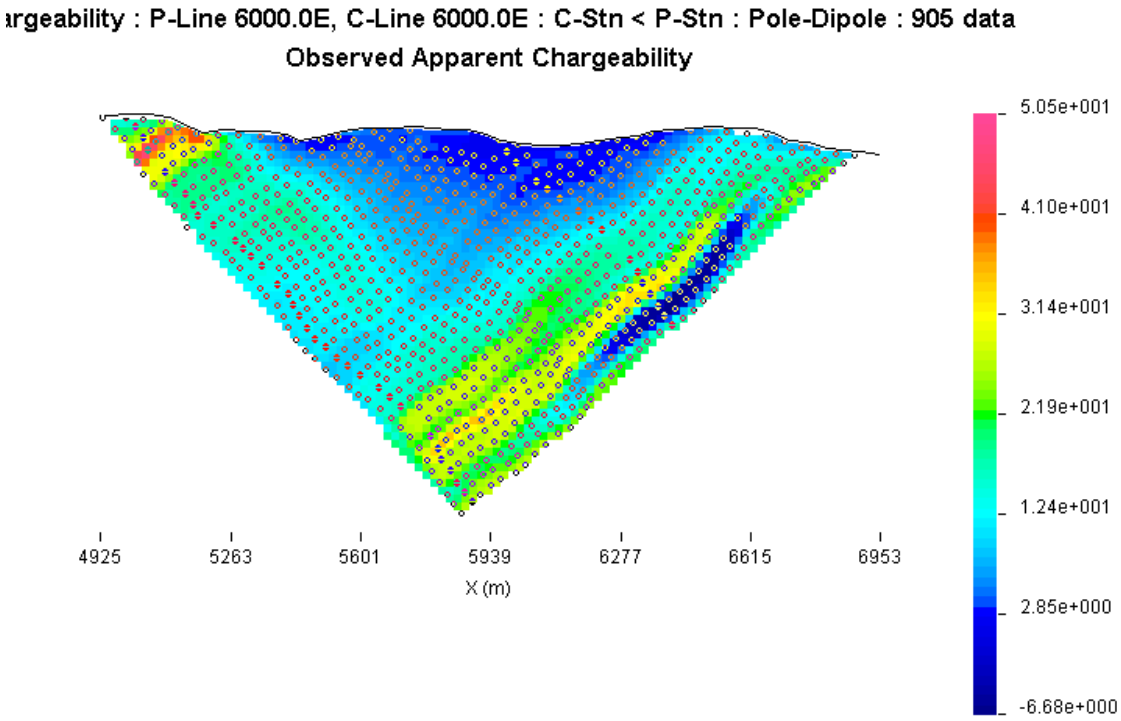
rgeability : P-Line 6000.0E, C-Line 6000.0E : C-Stn < P-Stn : Pole-Dipole : 905 data
Observed Apparent Chargeability
5.05e+001
4.10e+001
3.14e+001
2.19e+001
1.24e+001
2.85e+000
-6.68e+000
4925
5263
5601
5939
6277
6615
6953
X (m)

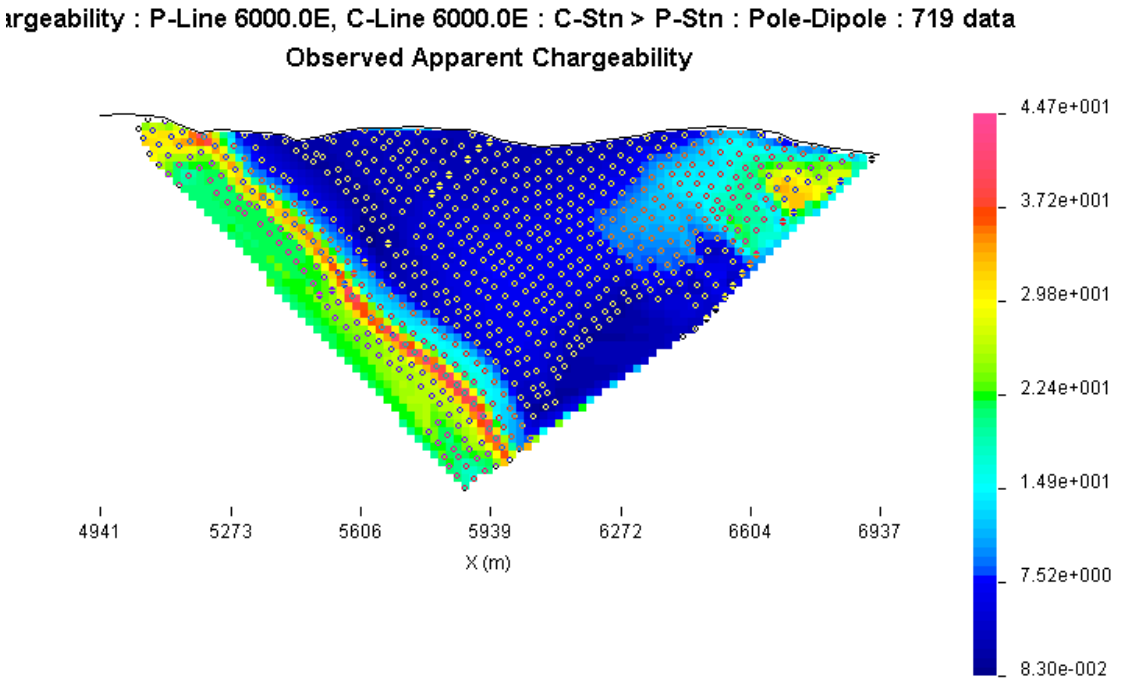
rgeability : P-Line 6000.0E, C-Line 6000.0E : C-Stn > P-Stn : Pole-Dipole : 719 data
Observed Apparent Chargeability
4.47e+001
3.72e+001
2.98e+001
2.24e+001
1.49e+001
7.52e+000
8.30e-002
4941
5273
5606
5939
6272
6604
6937
X (m)

otential : P-Line 7000.0E, C-Line 7000.0E : C-Stn < P-Stn : Pole-Dipole : 965 data

Observed Apparent Resistivity

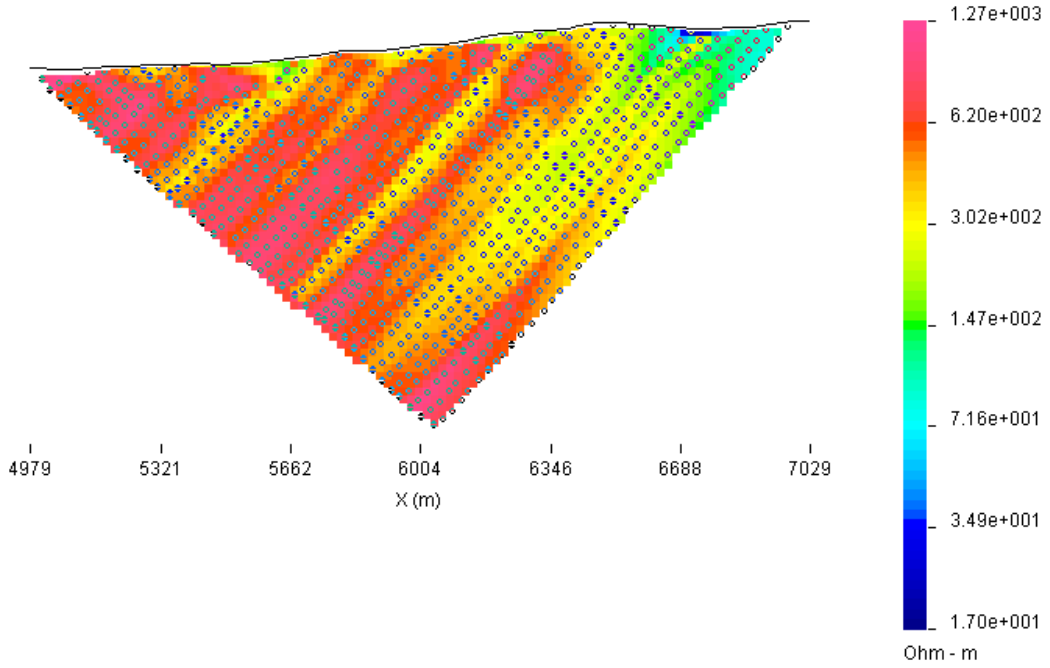

otential : P-Line 7000.0E, C-Line 7000.0E : C-Stn > P-Stn : Pole-Dipole : 910 data

Observed Apparent Resistivity

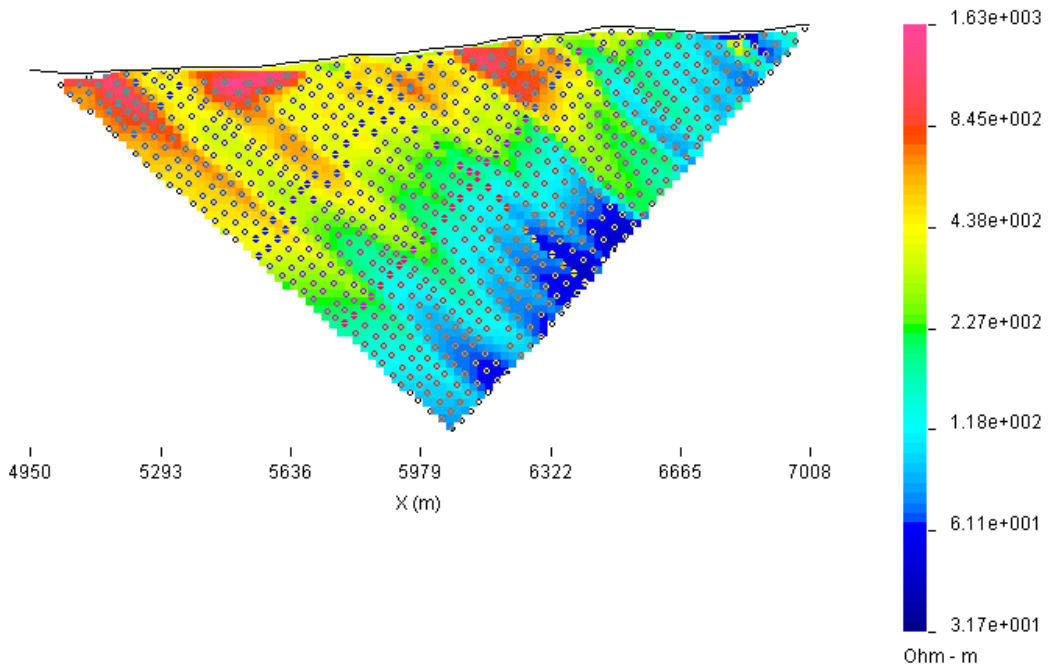

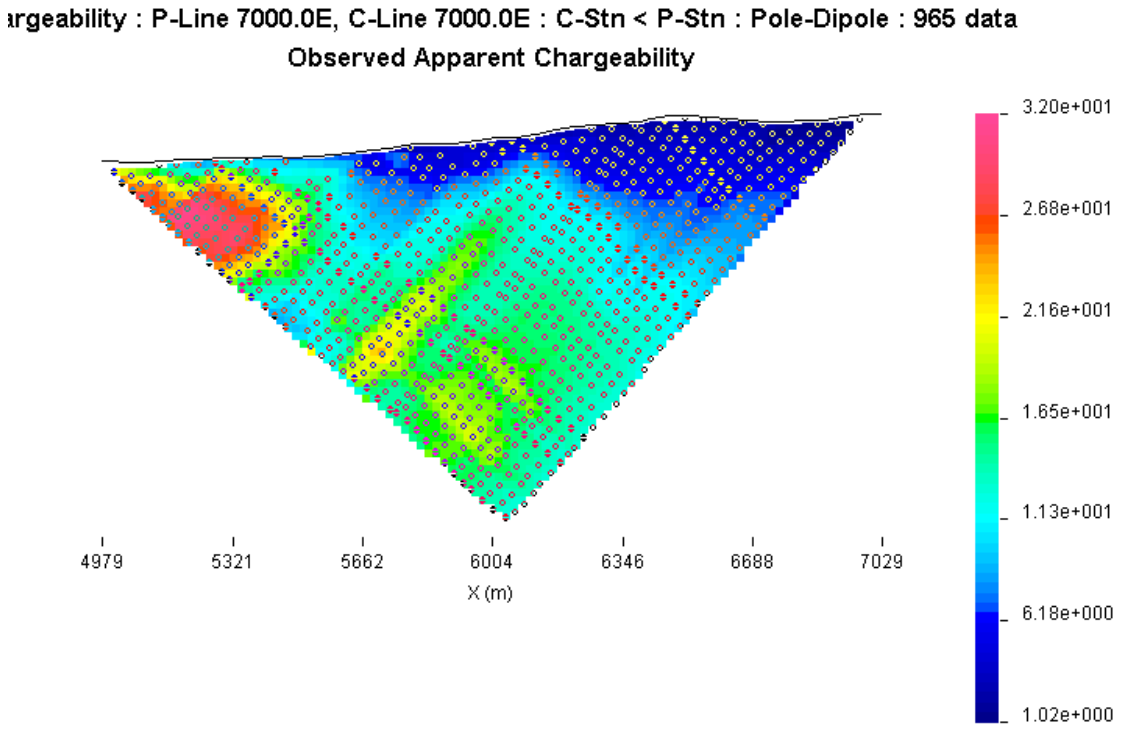
rgeability : P-Line 7000.0E, C-Line 7000.0E : C-Stn < P-Stn : Pole-Dipole : 965 data
Observed Apparent Chargeability
3.20e+001
2.68e+001
2.16e+001
1.65e+001
1.13e+001
6.18e+000
1.02e+000
4979
5321
5662
6004
6346
6688
7029
X (m)

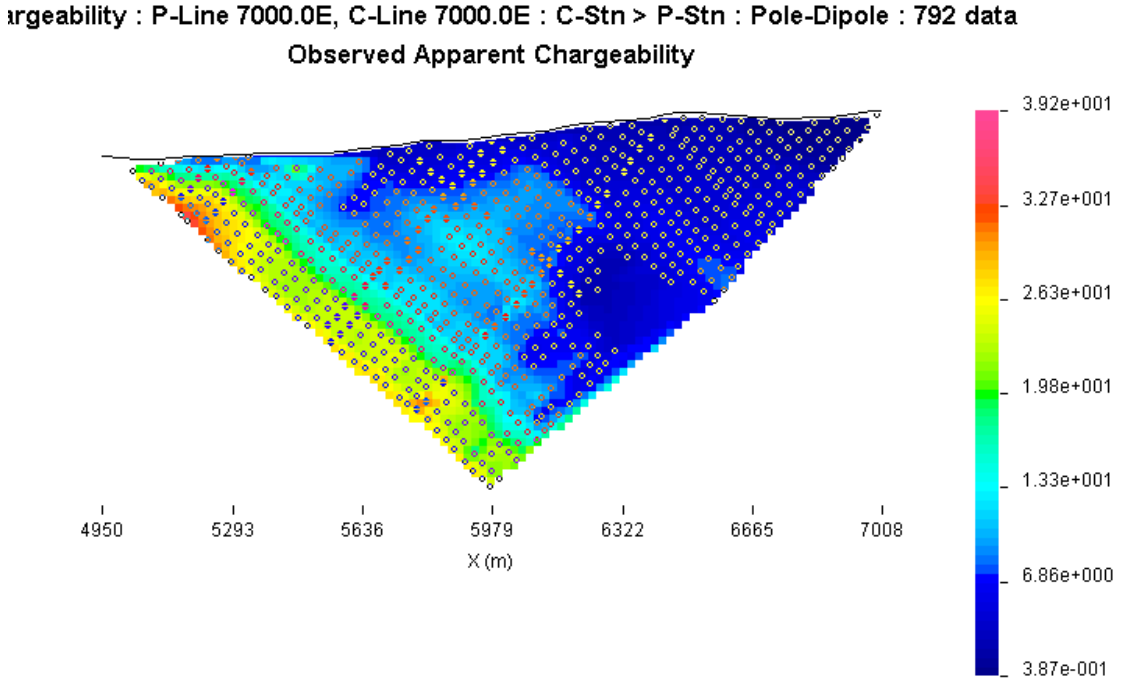
rgeability : P-Line 7000.0E, C-Line 7000.0E : C-Stn > P-Stn : Pole-Dipole : 792 data
Observed Apparent Chargeability
3.92e+001
3.27e+001
2.63e+001
1.98e+001
1.33e+001
6.86e+000
3.87e-001
4950
5293
5636
5979
6322
6665
7008
X (m)

INVERTED MODEL RESULTS

Line 1000E

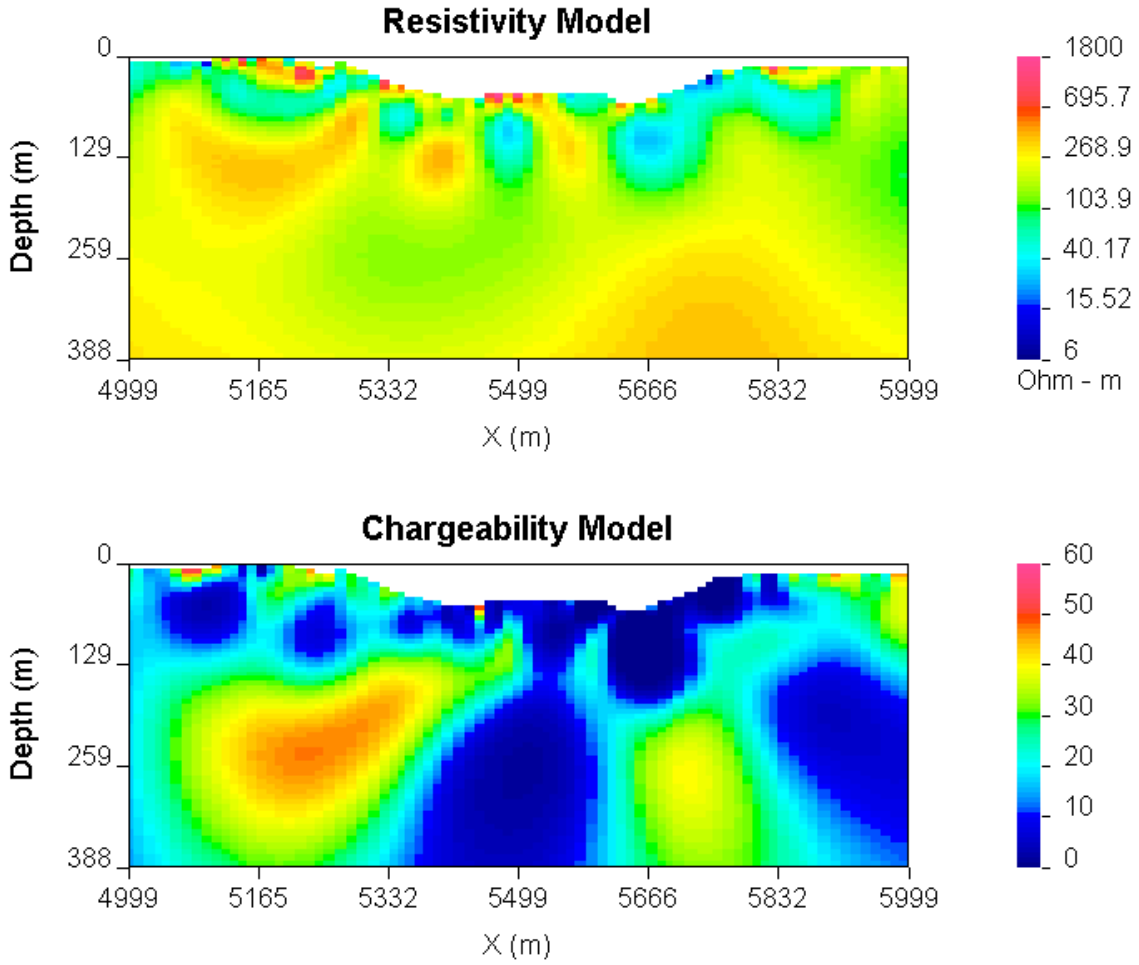

Line 2000E

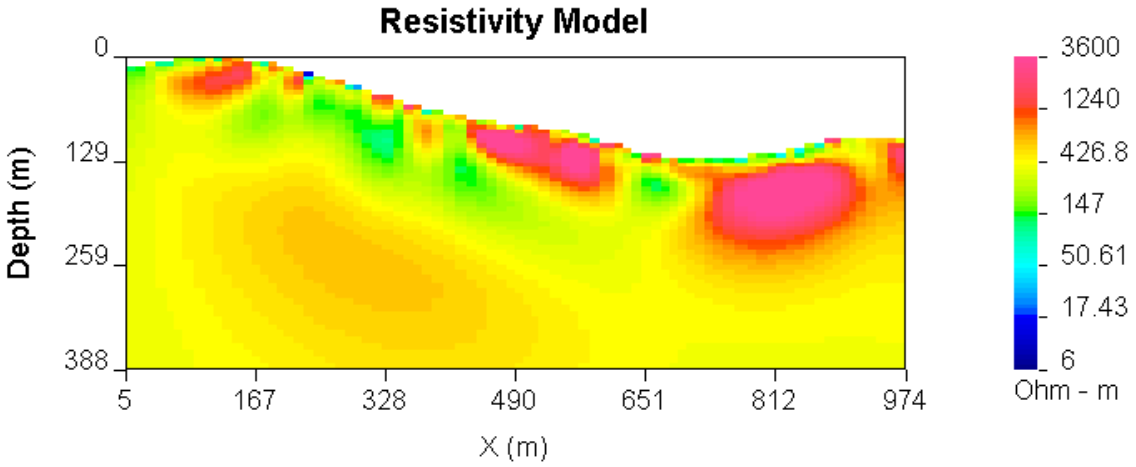

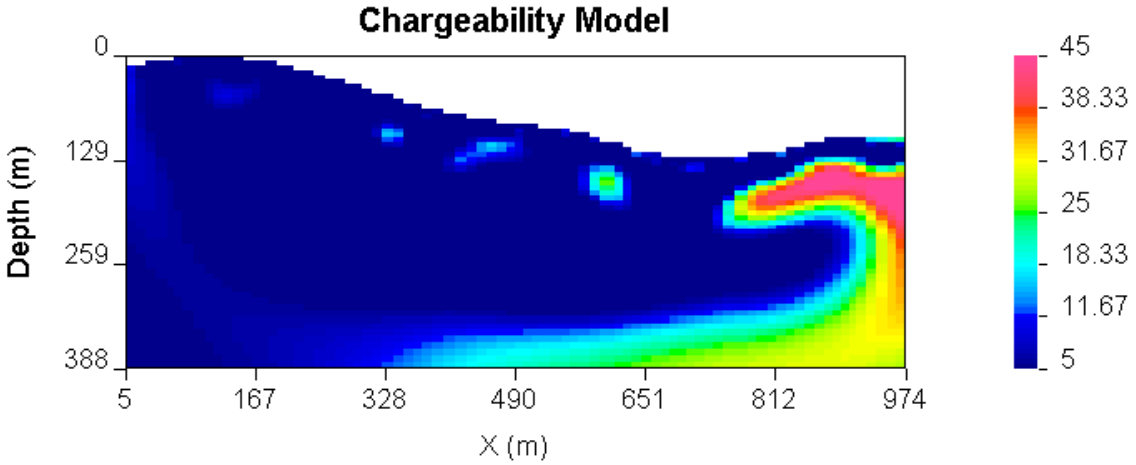

Line 3000E

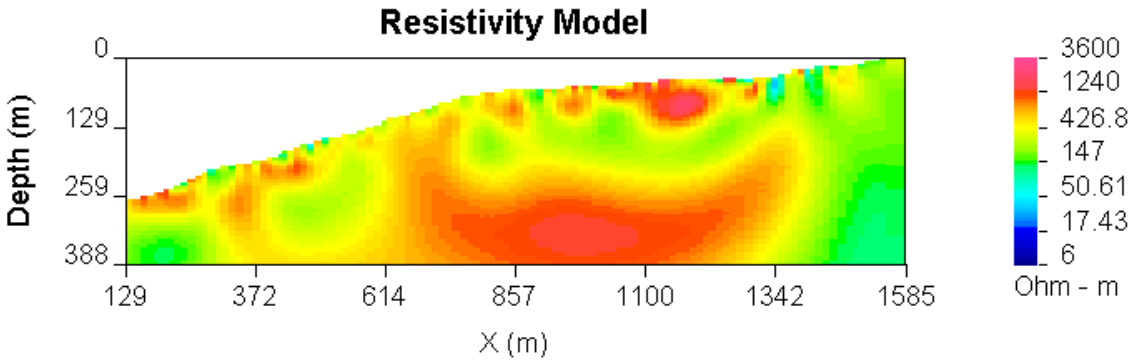

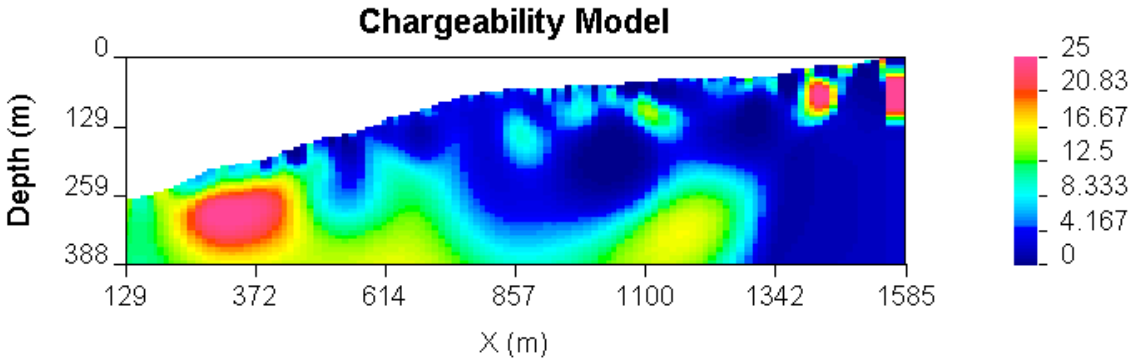
Chargeability Model
Depth (m)
0
129
259
388
129
372
614
857
1100
1342
1585
X (m)
25
20.83
16.67
12.5
8.333
4.167
0

Line 5000E

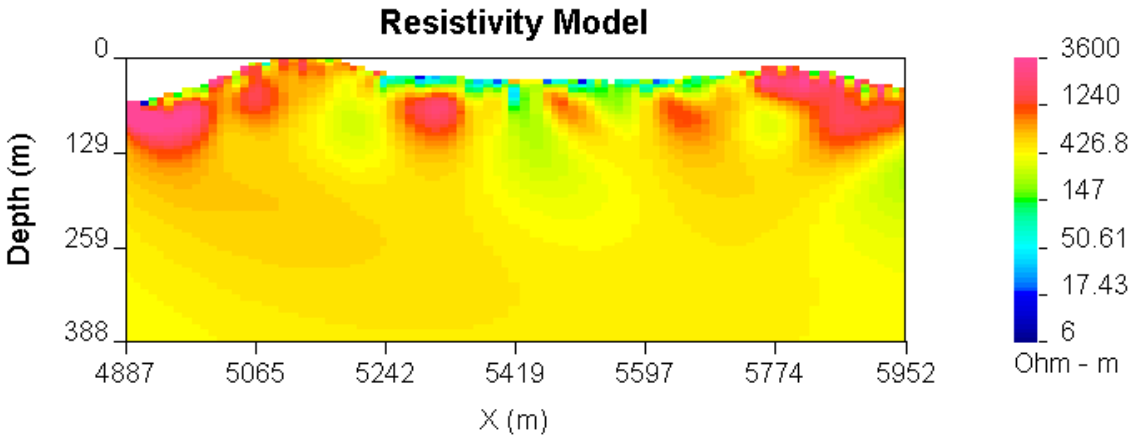
Resistivity Model
Depth (m)
0
129
259
388
4887
5065
5242
5419
5597
5774
5952
X (m)
3600
1240
426.8
147
50.61
17.43
6
Ohm - m

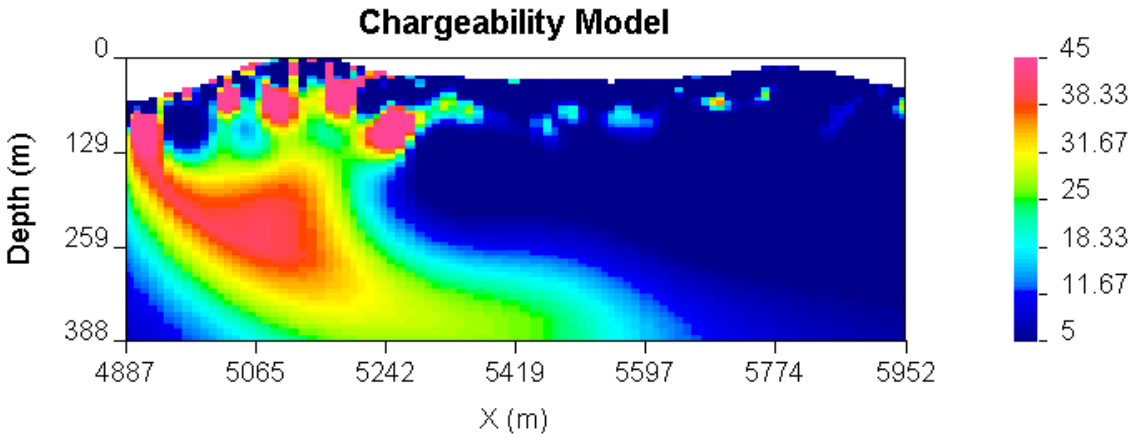
Chargeability Model
Depth (m)
0
129
259
388
4887
5065
5242
5419
5597
5774
5952
X (m)
45
38.33
31.67
25
18.33
11.67
5

Line 6000E

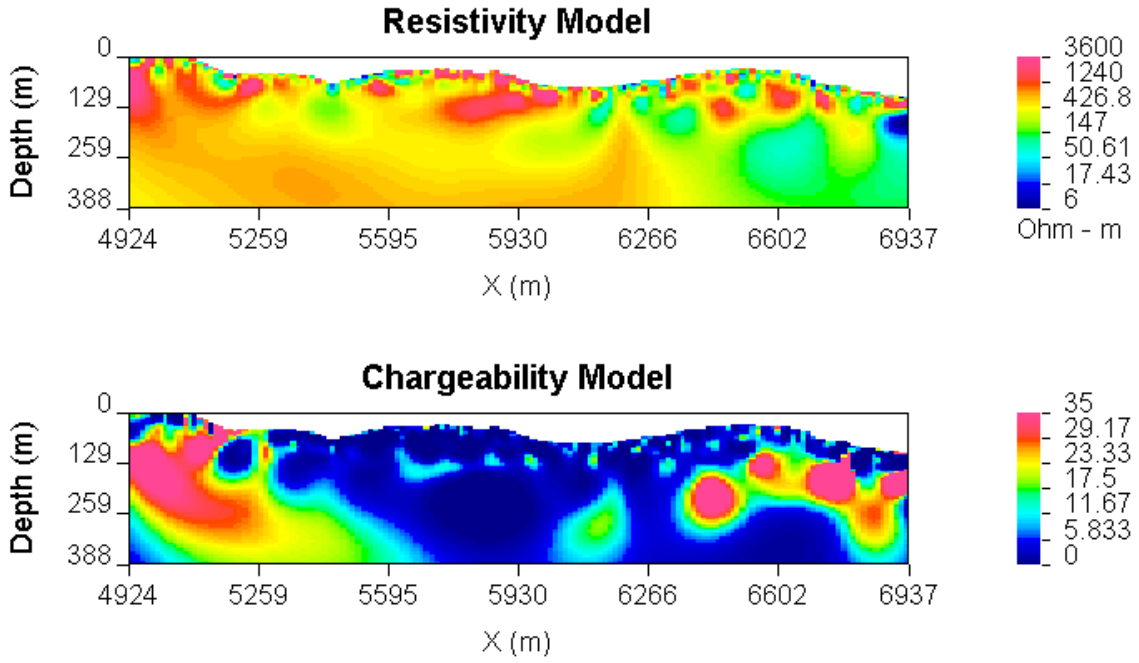

Line 7000E